Numerical methods and comparison for the nonlinear Dirac equation in the nonrelativistic limit regime

BAO WeiZhu[a], JIA XiaoWei[a], YIN Jia[b]

[a] *Department of Mathematics, National University of Singapore, Singapore 119076, Singapore*
[b] *NUS Graduate School for Integrative Sciences and Engineering (NGS), National University of Singapore, Singapore 117456, Singapore*

Abstract

We present and analyze several numerical methods for the discretization of the nonlinear Dirac equation in the nonrelativistic limit regime, involving a small dimensionless parameter $0 < \varepsilon \ll 1$ which is inversely proportional to the speed of light. In this limit regime, the solution is highly oscillatory in time, i.e. there are propagating waves with wavelength $O(\varepsilon^2)$ and $O(1)$ in time and space, respectively. We begin with four frequently used finite difference time domain (FDTD) methods and establish rigorously error estimates for the FDTD methods, which depend explicitly on the mesh size h and time step τ as well as the small parameter $0 < \varepsilon \leq 1$. Based on the error bounds, in order to obtain 'correct' numerical solutions in the nonrelativistic limit regime, i.e. $0 < \varepsilon \ll 1$, the FDTD methods share the same ε-scalability: $\tau = O(\varepsilon^3)$ and $h = O(\sqrt{\varepsilon})$. Then we propose and analyze two numerical methods for the discretization of the nonlinear Dirac equation by using the Fourier spectral discretization for spatial derivatives combined with the exponential wave integrator and time-splitting technique for temporal derivatives, respectively. Rigorous error bounds for the two numerical methods show that their ε-scalability is improved to $\tau = O(\varepsilon^2)$ and $h = O(1)$ when $0 < \varepsilon \ll 1$ compared with the FDTD methods. Extensive numerical results are reported to confirm our error estimates.

Keywords: nonlinear Dirac equation (NLDE), nonrelativistic limit regime, finite difference time domain method, exponential wave integrator spectral method, time splitting spectral method, ε-scalability

1. Introduction

In particle physics and/or relativistic quantum mechanics, the Dirac equation, which was derived by the British physicist Paul Dirac in 1928 [25, 26], is a relativistic wave equation for describing all spin-1/2 massive particles, such as electrons and positrons. It is consistent with both the principle of quantum mechanics and the theory of special relativity, and was the first theory to fully account for relativity in the context of quantum mechanics. It accounted for the fine details of the hydrogen spectrum in a completely rigorous way and provided the entailed explanation of spin as a consequence of the union of quantum mechanics and relativity – and the eventual discovery of the positron – represent one of the great triumphs of theoretical physics. Since the graphene was first produced in the lab in 2003 [1, 59], the Dirac equation has been extensively adopted to study theoretically the structures and/or dynamical properties of graphene and graphite as well as two dimensional (2D) materials [1, 30, 59]. Recently, the Dirac equation has also been adopted to study the relativistic effects in molecules in super intense lasers, e.g. attosecond lasers [32, 33] and the motion of nucleons in the covariant density function theory in the relativistic framework [62, 52].

Email addresses: matbaowz@nus.edu.sg (BAO WeiZhu), A0068124@nus.edu.sg (JIA XiaoWei), e0005518@u.nus.edu (YIN Jia)
URL: http://www.math.nus.edu.sg/~bao/ (BAO WeiZhu)

The nonlinear Dirac equation (NLDE), which was proposed in 1938 [45], is a model of self-interacting Dirac fermions in quantum field theory [34, 36, 69, 73] and is widely considered as a toy model of self-interacting spinor fields in quantum physics [69, 73]. In fact, it has also been appeared in the Einstein-Cartan-Sciama-Kibble theory of gravity, which extends general relativity to matter with intrinsic angular momentum (spin) [44]. In the resulting field equations, the minimal coupling between the homogeneous torsion tensor and Dirac spinors generates an axial-axial, spin-spin interaction in fermionic matter, which becomes nonlinear (cubic) in the spinor field and significant only at extremely high densities. Recently, the NLDE has been adapted as a mean field model for Bose-Einstein condensates (BECs) [22, 39, 40] and/or cosmology [63]. In fact, the experimental advances in BECs and/or graphene as well as 2D materials have renewed extensively the research interests on the mathematical analysis and numerical simulations of the Dirac equation and/or the NLDE without/with electromagnetic potentials, especially the honeycomb lattice potential [2, 30, 31].

Consider the NLDE in three dimensions (3D) for describing the dynamics of spin-1/2 self-interacting massive Dirac fermions within external time-dependent electromagnetic potentials [25, 34, 36, 69, 73, 39, 40]

$$i\hbar\partial_t\Psi = \Big[-ic\hbar\sum_{j=1}^{3}\alpha_j\partial_j + mc^2\beta\Big]\Psi + e\Big[V(t,\mathbf{x})I_4 - \sum_{j=1}^{3}A_j(t,\mathbf{x})\alpha_j\Big]\Psi + \mathbf{F}(\Psi)\Psi, \quad \mathbf{x}\in\mathbb{R}^3, \tag{1.1}$$

where $i=\sqrt{-1}$, t is time, $\mathbf{x}=(x_1,x_2,x_3)^T\in\mathbb{R}^3$ (equivalently written as $\mathbf{x}=(x,y,z)^T$) is the spatial coordinate vector, $\partial_k=\frac{\partial}{\partial x_k}$ $(k=1,2,3)$, $\Psi:=\Psi(t,\mathbf{x})=(\psi_1(t,\mathbf{x}),\psi_2(t,\mathbf{x}),\psi_3(t,\mathbf{x}),\psi_4(t,\mathbf{x}))^T\in\mathbb{C}^4$ is the complex-valued vector wave function of the "spinorfield". I_n is the $n\times n$ identity matrix for $n\in\mathbb{N}$, $V:=V(t,\mathbf{x})$ is the real-valued electrical potential and $\mathbf{A}:=\mathbf{A}(t,\mathbf{x})=(A_1(t,\mathbf{x}),A_2(t,\mathbf{x}),A_3(t,\mathbf{x}))^T$ is the real-valued magnetic potential vector, and hence the electric field is given by $\mathbf{E}(t,\mathbf{x})=-\nabla V-\partial_t\mathbf{A}$ and the magnetic field is given by $\mathbf{B}(t,\mathbf{x})=\operatorname{curl}\mathbf{A}=\nabla\times\mathbf{A}$. Different cubic nonlinearities have been proposed and studied for the NLDE (1.1) from different applications [34, 36, 69, 73, 39, 40, 80]. For the simplicity of notations, here we take $\mathbf{F}(\Psi)=g_1\,(\Psi^*\beta\Psi)\,\beta+g_2|\Psi|^2I_4$ with $g_1,g_2\in\mathbb{R}$ two constants and $\Psi^*=\overline{\Psi}^T$, while $\overline{f}$ denotes the complex conjugate of f, which is motivated from the so-called Soler model, e.g. $g_2=0$ and $g_1\neq 0$, in quantum field theory [34, 36, 69, 73] and BECs with a chiral confinement and/or spin-orbit coupling, e.g. $g_1=0$ and $g_2\neq 0$ [22, 39, 40]. We remark here that our numerical methods and their error estimates can be easily extended to the NLDE with other nonlinearities [73, 63, 64]. The physical constants are: c for the speed of light, m for the particle's rest mass, $\hbar$ for the Planck constant and e for the unit charge. In addition, the 4×4 matrices α_1, α_2, α_3 and β are defined as

$$\alpha_1=\begin{pmatrix}\mathbf{0}&\sigma_1\\ \sigma_1&\mathbf{0}\end{pmatrix},\qquad \alpha_2=\begin{pmatrix}\mathbf{0}&\sigma_2\\ \sigma_2&\mathbf{0}\end{pmatrix},\qquad \alpha_3=\begin{pmatrix}\mathbf{0}&\sigma_3\\ \sigma_3&\mathbf{0}\end{pmatrix},\qquad \beta=\begin{pmatrix}I_2&\mathbf{0}\\ \mathbf{0}&-I_2\end{pmatrix}, \tag{1.2}$$

with σ_1, σ_2, σ_3 (equivalently written σ_x, σ_y, σ_z) being the Pauli matrices defined as

$$\sigma_1=\begin{pmatrix}0&1\\ 1&0\end{pmatrix},\qquad \sigma_2=\begin{pmatrix}0&-i\\ i&0\end{pmatrix},\qquad \sigma_3=\begin{pmatrix}1&0\\ 0&-1\end{pmatrix}. \tag{1.3}$$

Similar to the Dirac equation [11], by a proper nondimensionalization (with the choice of x_s, $t_s=\frac{mx_s^2}{\hbar}$, $A_s=\frac{mv^2}{e}$ and $\psi_s=x_s^{-3/2}$ as the dimensionless length unit, time unit, potential unit and spinor field unit, respectively) and dimension reduction [11], we can obtain the dimensionless NLDE in d-dimensions $(d=3,2,1)$

$$i\partial_t\Psi = \Big[-\frac{i}{\varepsilon}\sum_{j=1}^{d}\alpha_j\partial_j + \frac{1}{\varepsilon^2}\beta\Big]\Psi + \Big[V(t,\mathbf{x})I_4 - \sum_{j=1}^{d}A_j(t,\mathbf{x})\alpha_j\Big]\Psi + \mathbf{F}(\Psi)\Psi, \quad \mathbf{x}\in\mathbb{R}^d, \tag{1.4}$$

where ε is a dimensionless parameter inversely proportional to the speed of light given by

$$0<\varepsilon:=\frac{x_s}{t_s\,c}=\frac{v}{c}\leq 1, \tag{1.5}$$

with $v = \frac{x_s}{t_s}$ the wave speed, and

$$\mathbf{F}(\Psi) = \lambda_1 \left(\Psi^* \beta \Psi\right) \beta + \lambda_2 |\Psi|^2 I_4, \qquad \Psi \in \mathbb{C}^4, \tag{1.6}$$

with $\lambda_1 = \frac{g_1}{m v^2 x_s^3} \in \mathbb{R}$ and $\lambda_2 = \frac{g_2}{m v^2 x_s^3} \in \mathbb{R}$ two dimensionless constants for the interaction strength.

For the dynamics, the initial condition is given as

$$\Psi(t = 0, \mathbf{x}) = \Psi_0(\mathbf{x}), \qquad \mathbf{x} \in \mathbb{R}^d.$$

The NLDE (1.4) is dispersive and time symmetric [79]. Introducing the position density ρ_j for the j-component ($j = 1, 2, 3, 4$) and the total density ρ as well as the current density $\mathbf{J}(t, \mathbf{x}) = (J_1(t, \mathbf{x}), J_2(t, \mathbf{x}), J_3(t, \mathbf{x}))^T$

$$\rho(t, \mathbf{x}) = \sum_{j=1}^{4} \rho_j(t, \mathbf{x}) = \Psi^* \Psi, \quad \rho_j(t, \mathbf{x}) = |\psi_j(t, \mathbf{x})|^2, \quad 1 \le j \le 4; \quad J_l(t, \mathbf{x}) = \frac{1}{\varepsilon} \Psi^* \alpha_l \Psi, \quad l = 1, 2, 3, \tag{1.7}$$

then the following conservation law can be obtained from the NLDE (1.4)

$$\partial_t \rho(t, \mathbf{x}) + \nabla \cdot \mathbf{J}(t, \mathbf{x}) = 0, \qquad \mathbf{x} \in \mathbb{R}^d, \quad t \ge 0. \tag{1.8}$$

Thus the NLDE (1.4) conserves the total mass as

$$\|\Psi(t, \cdot)\|^2 := \int_{\mathbb{R}^d} |\Psi(t, \mathbf{x})|^2 \, d\mathbf{x} = \int_{\mathbb{R}^d} \sum_{j=1}^{4} |\psi_j(t, \mathbf{x})|^2 \, d\mathbf{x} \equiv \|\Psi(0, \cdot)\|^2 = \|\Psi_0\|^2, \qquad t \ge 0. \tag{1.9}$$

If the electric potential V is perturbed by a constant, e.g. $V(t, \mathbf{x}) \to V(t, \mathbf{x}) + V^0$ with V^0 being a real constant, then the solution $\Psi(t, \mathbf{x}) \to e^{-iV^0 t} \Psi(t, \mathbf{x})$ which implies the density of each component ρ_j ($j = 1, 2, 3, 4$) and the total density ρ unchanged. When $d = 1$, if the magnetic potential A_1 is perturbed by a constant, e.g. $A_1(t, \mathbf{x}) \to A_1(t, \mathbf{x}) + A_1^0$ with A_1^0 being a real constant, then the solution $\Psi(t, \mathbf{x}) \to e^{iA_1^0 t \alpha_1} \Psi(t, \mathbf{x})$ which implies the total density ρ unchanged; but this property is not valid when $d = 2, 3$. These properties are usually called as time transverse invariant. In addition, when the electromagnetic potentials are time-independent, i.e. $V(t, \mathbf{x}) = V(\mathbf{x})$ and $A_j(t, \mathbf{x}) = A_j(\mathbf{x})$ for $j = 1, 2, 3$, the following energy functional is also conserved

$$\begin{aligned} E(t) &:= \int_{\mathbb{R}^d} \left[-\frac{i}{\varepsilon} \sum_{j=1}^{d} \Psi^* \alpha_j \partial_j \Psi + \frac{1}{\varepsilon^2} \Psi^* \beta \Psi + V(\mathbf{x}) |\Psi|^2 + G(\Psi) - \sum_{j=1}^{d} A_j(\mathbf{x}) \Psi^* \alpha_j \Psi \right] d\mathbf{x} \\ &\equiv E(0), \qquad t \ge 0, \end{aligned} \tag{1.10}$$

where

$$G(\Psi) = \frac{\lambda_1}{2} \left(\Psi^* \beta \Psi\right)^2 + \frac{\lambda_2}{2} |\Psi|^4, \qquad \Psi \in \mathbb{C}^4. \tag{1.11}$$

Furthermore, if the external electromagnetic potentials are constants, i.e. $V(t, \mathbf{x}) \equiv V^0$ and $A_j(t, \mathbf{x}) \equiv A_j^0$ for $j = 1, 2, 3$, the NLDE (1.4) admits the plane wave solution as $\Psi(t, \mathbf{x}) = \mathbf{B} \, e^{i(\mathbf{k} \cdot \mathbf{x} - \omega t)}$, where the time frequency ω, amplitude vector $\mathbf{B} \in \mathbb{R}^4$ and spatial wave number $\mathbf{k} = (k_1, \ldots, k_d)^T \in \mathbb{R}^d$ satisfy

$$\omega \mathbf{B} = \left[\sum_{j=1}^{d} \left(\frac{k_j}{\varepsilon} - A_j^0 \right) \alpha_j + \frac{1}{\varepsilon^2} \beta + V^0 I_4 + \lambda_1 \left(\mathbf{B}^* \beta \mathbf{B}\right) \beta + \lambda_2 |\mathbf{B}|^2 I_4 \right] \mathbf{B}, \tag{1.12}$$

which immediately implies the *dispersion relation* of the NLDE (1.4) as

$$\omega := \omega(\mathbf{k}, \mathbf{B}) = V^0 + \lambda_2 |\mathbf{B}|^2 \pm \frac{1}{\varepsilon^2} \sqrt{\left[1 + \varepsilon^2 \lambda_1 \left(\mathbf{B}^* \beta \mathbf{B}\right)\right]^2 + \varepsilon^2 \left|\mathbf{k} - \varepsilon \mathbf{A}^0\right|^2}, \qquad \mathbf{k} \in \mathbb{R}^d. \tag{1.13}$$

Again, similar to the Dirac equation [11], in several applications in one dimension (1D) and two dimensions (2D), the NLDE (1.4) can be simplified to the following NLDE in d-dimensions ($d = 1, 2$) with $\Phi := \Phi(t, \mathbf{x}) = (\phi_1(t, \mathbf{x}), \phi_2(t, \mathbf{x}))^T \in \mathbb{C}^2$ [34, 36, 69]

$$i\partial_t \Phi = \Big[-\frac{i}{\varepsilon}\sum_{j=1}^{d}\sigma_j\partial_j + \frac{1}{\varepsilon^2}\sigma_3\Big]\Phi + \Big[V(t,\mathbf{x})I_2 - \sum_{j=1}^{d}A_j(t,\mathbf{x})\sigma_j\Big]\Phi + \mathbf{F}(\Phi)\Phi, \quad \mathbf{x}\in\mathbb{R}^d, \tag{1.14}$$

where

$$\mathbf{F}(\Phi) = \lambda_1\left(\Phi^*\sigma_3\Phi\right)\sigma_3 + \lambda_2|\Phi|^2 I_2, \qquad \Phi \in \mathbb{C}^2, \tag{1.15}$$

with $\lambda_1 \in \mathbb{R}$ and $\lambda_2 \in \mathbb{R}$ two dimensionless constants for the interaction strength. Again, the initial condition for dynamics is given as

$$\Phi(t = 0, \mathbf{x}) = \Phi_0(\mathbf{x}), \qquad \mathbf{x} \in \mathbb{R}^d. \tag{1.16}$$

The NLDE (1.14) is dispersive and time symmetric. By introducing the position density ρ_j for the j-th component ($j = 1, 2$) and the total density ρ as well as the current density $\mathbf{J}(t, \mathbf{x}) = (J_1(t, \mathbf{x}), J_2(t, \mathbf{x}))^T$

$$\rho(t,\mathbf{x}) = \sum_{j=1}^{2}\rho_j(t,\mathbf{x}) = \Phi^*\Phi, \quad \rho_j(t,\mathbf{x}) = |\phi_j(t,\mathbf{x})|^2, \quad J_j(t,\mathbf{x}) = \frac{1}{\varepsilon}\Phi^*\sigma_j\Phi, \quad j = 1, 2, \tag{1.17}$$

the conservation law (1.8) is also satisfied [20]. In addition, the Dirac equation (1.14) conserves the total mass as

$$\|\Phi(t,\cdot)\|^2 := \int_{\mathbb{R}^d}|\Phi(t,\mathbf{x})|^2\,d\mathbf{x} = \int_{\mathbb{R}^d}\sum_{j=1}^{2}|\phi_j(t,\mathbf{x})|^2\,d\mathbf{x} \equiv \|\Phi(0,\cdot)\|^2 = \|\Phi_0\|^2, \qquad t \geq 0. \tag{1.18}$$

Again, if the electric potential V is perturbed by a constant, e.g. $V(t, \mathbf{x}) \to V(t, \mathbf{x}) + V^0$ with V^0 being a real constant, the solution $\Phi(t, \mathbf{x}) \to e^{-iV^0 t}\Phi(t, \mathbf{x})$ which implies the density of each component ρ_j ($j = 1, 2$) and the total density ρ unchanged. When $d = 1$, if the magnetic potential A_1 is perturbed by a constant, e.g. $A_1(t, \mathbf{x}) \to A_1(t, \mathbf{x}) + A_1^0$ with A_1^0 being a real constant, the solution $\Phi(t, \mathbf{x}) \to e^{iA_1^0 t\sigma_1}\Phi(t, \mathbf{x})$ implying the total density ρ unchanged; but this property is not valid when $d = 2$. When the electromagnetic potentials are time-independent, i.e. $V(t, \mathbf{x}) = V(\mathbf{x})$ and $A_j(t, \mathbf{x}) = A_j(\mathbf{x})$ for $j = 1, 2$, the following energy functional is also conserved

$$\begin{aligned} E(t) &:= \int_{\mathbb{R}^d}\left(-\frac{i}{\varepsilon}\sum_{j=1}^{d}\Phi^*\sigma_j\partial_j\Phi + \frac{1}{\varepsilon^2}\Phi^*\sigma_3\Phi + V(\mathbf{x})|\Phi|^2 - \sum_{j=1}^{d}A_j(\mathbf{x})\Phi^*\sigma_j\Phi + G(\Phi)\right)d\mathbf{x} \\ &\equiv E(0), \qquad t \geq 0, \end{aligned} \tag{1.19}$$

where

$$G(\Phi) = \frac{\lambda_1}{2}\left(\Phi^*\sigma_3\Phi\right)^2 + \frac{\lambda_2}{2}|\Phi|^4, \qquad \Phi \in \mathbb{C}^2. \tag{1.20}$$

Furthermore, if the external electromagnetic potentials are constants, i.e. $V(t, \mathbf{x}) \equiv V^0$ and $A_j(t, \mathbf{x}) \equiv A_j^0$ for $j = 1, 2$, the Dirac equation (1.14) admits the plane wave solution as $\Phi(t, \mathbf{x}) = \mathbf{B}\,e^{i(\mathbf{k}\cdot\mathbf{x}-\omega t)}$, where the time frequency ω, amplitude vector $\mathbf{B} \in \mathbb{R}^2$ and spatial wave number $\mathbf{k} = (k_1, \ldots, k_d)^T \in \mathbb{R}^d$ satisfy

$$\omega\mathbf{B} = \Big[\sum_{j=1}^{d}\left(\frac{k_j}{\varepsilon} - A_j^0\right)\sigma_j + \frac{1}{\varepsilon^2}\sigma_3 + V^0 I_2 + \lambda_1\left(\mathbf{B}^*\sigma_3\mathbf{B}\right)\sigma_3 + \lambda_2|\mathbf{B}|^2 I_2\Big]\mathbf{B}. \tag{1.21}$$

which immediately implies the *dispersion relation* of the NLDE (1.14) as

$$\omega := \omega(\mathbf{k}, \mathbf{B}) = V^0 + \lambda_2|\mathbf{B}|^2 \pm \frac{1}{\varepsilon^2}\sqrt{\left[1 + \varepsilon^2\lambda_1\left(\mathbf{B}^*\sigma_3\mathbf{B}\right)\right]^2 + \varepsilon^2\left|\mathbf{k} - \varepsilon\mathbf{A}^0\right|^2}, \qquad \mathbf{k} \in \mathbb{R}^d. \tag{1.22}$$

For the NLDE (1.4) (or (1.14)) with $\varepsilon = 1$, i.e. $O(1)$-speed of light regime, there are extensive analytical and numerical results in the literatures. For the existence and multiplicity of bound states and/or standing wave solutions, we refer to [6, 7, 17, 21, 27, 28, 29, 49] and references therein. Particularly, when $d = 1$, $\varepsilon = 1$, $V(t, x) \equiv 0$ and $A_1(t, x) \equiv 0$ in (1.14) and $\lambda_1 = -1$ and $\lambda_2 = 0$ in (1.15), the NLDE (1.14) admits soliton solutions which was given explicitly in [23, 36, 41, 50, 55, 61, 71, 72]. For the numerical methods and comparison such as the finite difference time domain (FDTD) methods [20, 43, 60], time-splitting Fourier spectral (TSFP) methods [16, 19, 24, 47] and Runge-Kutta discontinuous Galerkin methods [66, 76, 79], we refer to [16, 19, 20, 24, 43, 46, 47, 60, 65, 67] and references therein. However, for the NLDE (1.4) (or (1.14)) with $0 < \varepsilon \ll 1$, i.e. nonrelativistic limit regime (or the scaled speed of light goes to infinity), the analysis and efficient computation of the NLDE (1.4) (or (1.14)) are mathematically rather complicated issues. The main difficulty is due to that the solution is highly oscillatory in time and the corresponding energy functionals (1.10) and (1.19) are indefinite [18, 29] and become unbounded when $\varepsilon \to 0$. For the Dirac equation, i.e. $\mathbf{F}(\Psi) \equiv 0$ in (1.6) (or $\mathbf{F}(\Phi) \equiv 0$ in (1.15)), there are extensive mathematical analysis of the (semi)-nonrelativistic limits [48, 18, 38, 54, 78]. For the NLDE (1.4) (or (1.14)), similar analysis of the nonrelativistic limits has been done in [35, 58]. These rigorous analytical results show that the solution propagates waves with wavelength $O(\varepsilon^2)$ and $O(1)$ in time and space, respectively, when $0 < \varepsilon \ll 1$. In fact, the oscillatory structure of the solution of the NLDE (1.4) (or (1.14)) when $0 < \varepsilon \ll 1$ can be formally observed from its dispersion relation (1.12) (or (1.21)). To illustrate this further, Figure 1.1 shows the solution of the NLDE (1.14) with $d = 1$, $V(t, x) = \frac{1-x}{1+x^2}$, $A_1(t, x) = \frac{(1+x)^2}{1+x^2}$, $\lambda_1 = -1$, $\lambda_2 = 0$ and $\Phi_0(x) = \big(\exp(-x^2/2), \exp(-(x-1)^2/2)\big)^T$ for different ε.

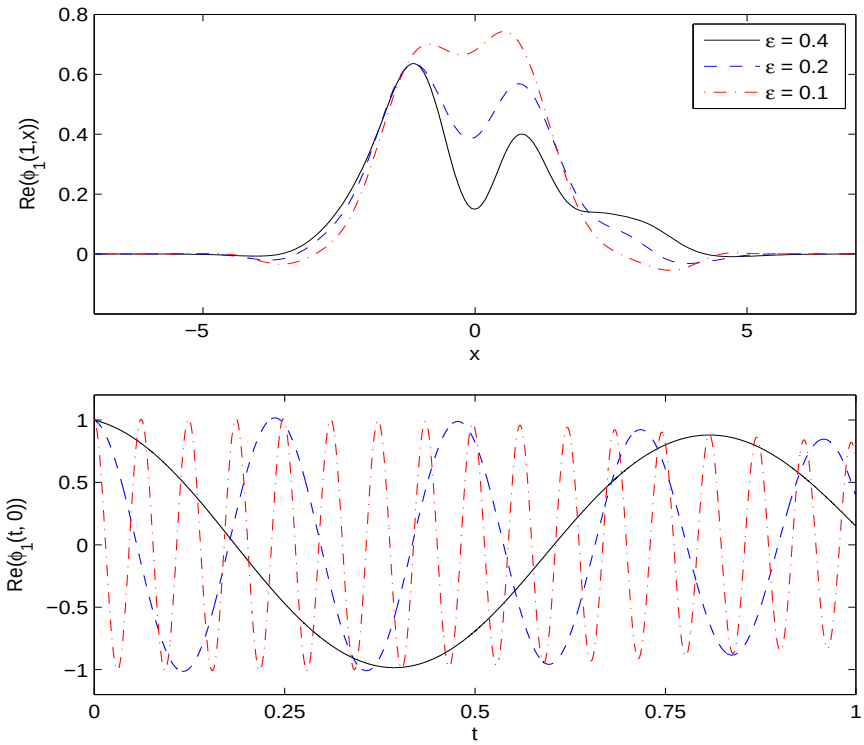

Figure 1.1: The solution $\phi_1(t = 1, x)$ and $\phi_1(t, x = 0)$ of the NLDE (1.14) with $d = 1$ for different ε. $\mathrm{Re}(f)$ denotes the real part of f.

The highly oscillatory nature of the solution of (1.4) (or (1.14)) causes severe numerical burdens in practical computation, making the numerical approximation of (1.4) (or (1.14)) extremely challenging and costly in the nonrelativistic regime $0 < \varepsilon \ll 1$. Recently, we compared the spatial/temporal resolution in

term of ε and established rigorous error estimates of the FDTD methods, TSFP methods for the Dirac equation in the nonrelativistic limit regime [11]. To our knowledge, so far there are few results on the numerics of the NLDE in the nonrelativistic limit regime. The aim of this paper is to study the efficiency of the frequently used FDTD and TSFP methods applied to the NLDE in the nonrelativistic limit regime, to propose the exponential wave integrator Fourier pseudospectral (EWI-FP) method and to compare their resolution capacities in this regime. We start with the detailed analysis on the convergence of several standard implicit/semi-implicit/explicit FDTD methods [11]. Here we pay particular attention to how the error bounds depend explicitly on the small parameter ε in addition to the mesh size h and time step τ. Based on the estimates, in order to obtain 'correct' numerical approximations when $0 < \varepsilon \ll 1$, the meshing strategy requirement (ε-scalability) for those frequently used FDTD methods is: $h = O(\sqrt{\varepsilon})$ and $\tau = O(\varepsilon^3)$, which suggests that the standard FDTD methods are computationally expensive for the NLDE (1.4) (or (1.14)) as $0 < \varepsilon \ll 1$. To relax the ε-scalability, we then propose the EWI-FP method and compare it with the TSFP method, whose ε-scalability are optimal for both time and space in view of the inherent oscillatory nature. The key ideas of the EWI-FP are: (i) to apply the Fourier pseudospectral discretization for spatial derivatives; and (ii) to adopt the exponential wave integrator (EWI) for integrating the ordinary differential equations (ODEs) in phase space [37, 42] which was well demonstrated in the literatures that it has favorable properties compared to standard time integrators for oscillatory differential equations [37, 42]. Rigorous error estimates show that the ε-scalability of the EWI-FP method is $h = O(1)$, and $\tau = O(\varepsilon^2)$ for the NLDE with external electromagnetic potentials, meanwhile, the ε-scalability of the TSFP method is $h = O(1)$ and $\tau = O(\varepsilon^2)$. Thus, the EWI-FP and TSFP offer compelling advantages over commonly used FDTD methods for the NLDE in temporal and spatial resolution when $0 < \varepsilon \ll 1$.

The rest of this paper is organized as follows. In Section 2, several second-order FDTD methods are reviewed and their convergence are analyzed in the nonrelativistic limit regime. In Section 3, an EWI-FP method is proposed and analyzed rigorously. In Section 4, a TSFP method is reviewed and analyzed rigorously. In Section 5, numerical comparison results are reported. Finally, some concluding remarks are drawn in Section 6. The mathematical proofs of the error estimates are given in the Appendices. Throughout the paper, we adopt the standard notations of Sobolev spaces, use the notation $p \lesssim q$ to represent that there exists a generic constant $C > 0$ which is independent of h, τ and ε such that $|p| \leq C\, q$.

2. FDTD methods and their analysis

In this section, we apply several conventional FDTD methods to the NLDE (1.14) (or (1.4)) with external electromagnetic field and analyze their stabilities and convergence in the nonrelativistic limit regime. For simplicity of notations, we shall only present the numerical methods and their analysis for (1.14) in 1D. Generalization to (1.4) and/or higher dimensions is straightforward and results remain valid without modifications. Similar to most works in the literatures for the analysis and computation of the NLDE (cf. [3, 5, 36, 46, 66, 76, 79] and references therein), in practical computation, we truncate the whole space problem onto an interval $\Omega = (a, b)$ with periodic boundary conditions, which is large enough such that the truncation error is negligible. In 1D, the NLDE (1.14) with periodic boundary conditions collapses to

$$i\partial_t \Phi = \left[-\frac{i}{\varepsilon}\sigma_1\partial_x + \frac{1}{\varepsilon^2}\sigma_3\right]\Phi + [V(t,x)I_2 - A_1(t,x)\sigma_1 + \mathbf{F}(\Phi)]\,\Phi, \quad x \in \Omega,\ t > 0, \tag{2.1}$$

$$\Phi(t,a) = \Phi(t,b), \quad \partial_x\Phi(t,a) = \partial_x\Phi(t,b), \quad t \geq 0, \qquad \Phi(0,x) = \Phi_0(x), \quad x \in \overline{\Omega}, \tag{2.2}$$

where $\Phi := \Phi(t,x) \in \mathbb{C}^2$, $\Phi_0(a) = \Phi_0(b)$, $\Phi_0'(a) = \Phi_0'(b)$ and $\mathbf{F}(\Phi)$ is given in (1.15).

2.1. FDTD methods

Choose mesh size $h := \Delta x = \frac{b-a}{M}$ with M being a positive integer, time step $\tau := \Delta t > 0$ and denote the grid points and time steps as:

$$x_j := a + jh, \quad j = 0, 1, \ldots, M; \qquad t_n := n\tau, \quad n = 0, 1, 2, \ldots.$$

Denote $X_M = \{U = (U_0, U_1, ..., U_M)^T \mid U_j \in \mathbb{C}^2, j = 0, 1, \ldots, M,\ U_0 = U_M\}$ and we always use $U_{-1} = U_{M-1}$ if it is involved. For any $U \in X_M$, we denote its Fourier representation as

$$U_j = \sum_{l=-M/2}^{M/2-1} \widetilde{U}_l\, e^{i\mu_l(x_j-a)} = \sum_{l=-M/2}^{M/2-1} \widetilde{U}_l\, e^{2ijl\pi/M}, \qquad j = 0, 1, \ldots, M, \tag{2.3}$$

where μ_l and $\widetilde{U}_l \in \mathbb{C}^2$ are defined as

$$\mu_l = \frac{2l\pi}{b-a}, \qquad \widetilde{U}_l = \frac{1}{M}\sum_{j=0}^{M-1} U_j\, e^{-2ijl\pi/M}, \qquad l = -\frac{M}{2}, \ldots, \frac{M}{2} - 1. \tag{2.4}$$

The standard l^2-norm in X_M is given as

$$\|U\|_{l^2}^2 = h\sum_{j=0}^{M-1} |U_j|^2, \qquad U \in X_M. \tag{2.5}$$

Let Φ_j^n be the numerical approximation of $\Phi(t_n, x_j)$ and $V_j^n = V(t_n, x_j)$, $V_j^{n+1/2} = V(t_n + \tau/2, x_j)$, $A_{1,j}^n = A_1(t_n, x_j)$, $A_{1,j}^{n+1/2} = A_1(t_n + \tau/2, x_j)$, $\mathbf{F}_j^n = \mathbf{F}(\Phi_j^n)$ and $\mathbf{F}_j^{n+1/2} = \frac{1}{2}\left[\mathbf{F}(\Phi_j^n) + \mathbf{F}(\Phi_j^{n+1})\right]$ for $0 \le j \le M$ and $n \ge 0$. Denote $\Phi^n = (\Phi_0^n, \Phi_1^n, \ldots, \Phi_M^n)^T \in X_M$ as the solution vector at $t = t_n$. Introduce the finite difference discretization operators for $j = 0, 1, \ldots, M-1$ and $n \ge 0$ as:

$$\delta_t^+\Phi_j^n = \frac{\Phi_j^{n+1} - \Phi_j^n}{\tau}, \qquad \delta_t\Phi_j^n = \frac{\Phi_j^{n+1} - \Phi_j^{n-1}}{2\tau}, \qquad \delta_x\Phi_j^n = \frac{\Phi_{j+1}^n - \Phi_{j-1}^n}{2h}, \qquad \Phi_j^{n+\frac{1}{2}} = \frac{\Phi_j^{n+1} + \Phi_j^n}{2}.$$

Here we consider several frequently used FDTD methods to discretize the NLDE (2.1) for $j = 0, 1, \ldots, M-1$.

I. Leap-frog finite difference (LFFD) method

$$i\delta_t\Phi_j^n = \left[-\frac{i}{\varepsilon}\sigma_1\delta_x + \frac{1}{\varepsilon^2}\sigma_3\right]\Phi_j^n + \left[V_j^n I_2 - A_{1,j}^n\sigma_1 + \mathbf{F}_j^n\right]\Phi_j^n, \qquad n \ge 1. \tag{2.6}$$

II. Semi-implicit finite difference (SIFD1) method

$$i\delta_t\Phi_j^n = -\frac{i}{\varepsilon}\sigma_1\delta_x\Phi_j^n + \left[\frac{1}{\varepsilon^2}\sigma_3 + V_j^n I_2 - A_{1,j}^n\sigma_1 + \mathbf{F}_j^n\right]\frac{\Phi_j^{n+1} + \Phi_j^{n-1}}{2}, \qquad n \ge 1. \tag{2.7}$$

III. Another semi-implicit finite difference (SIFD2) method

$$i\delta_t\Phi_j^n = \left[-\frac{i}{\varepsilon}\sigma_1\delta_x + \frac{1}{\varepsilon^2}\sigma_3\right]\frac{\Phi_j^{n+1} + \Phi_j^{n-1}}{2} + \left[V_j^n I_2 - A_{1,j}^n\sigma_1 + \mathbf{F}_j^n\right]\Phi_j^n, \quad n \ge 1. \tag{2.8}$$

IV. Crank-Nicolson finite difference (CNFD) method

$$i\delta_t^+\Phi_j^n = \left[-\frac{i}{\varepsilon}\sigma_1\delta_x + \frac{1}{\varepsilon^2}\sigma_3 + V_j^{n+1/2} I_2 - A_{1,j}^{n+1/2}\sigma_1 + \mathbf{F}_j^{n+1/2}\right]\Phi_j^{n+1/2}, \qquad n \ge 0. \tag{2.9}$$

The initial and boundary conditions in (2.2) are discretized as:

$$\Phi_M^{n+1} = \Phi_0^{n+1}, \quad \Phi_{-1}^{n+1} = \Phi_{M-1}^{n+1}, \quad n \ge 0, \qquad \Phi_j^0 = \Phi_0(x_j), \quad j = 0, 1, ..., M. \tag{2.10}$$

For the LFFD (2.6), SIFD1 (2.7) and SIFD2 (2.8), the first step can be approximated via the Taylor expansion and the NLDE (2.1) at $t = 0$ and (2.2) as

$$\Phi_j^1 = \Phi_j^0 + \tau \left[-\frac{1}{\tau} \sin\left(\frac{\tau}{\varepsilon}\right) \sigma_1 \delta_x \Phi_0(x_j) - i \left(\frac{1}{\tau} \sin\left(\frac{\tau}{\varepsilon^2}\right) \sigma_3 + V_j^0 I_2 - A_{1,j}^0 \sigma_1 + \mathbf{F}(\Phi_j^0) \right) \Phi_j^0 \right], \quad 0 \le j \le M-1. \tag{2.11}$$

In the above, we adapt $\frac{1}{\tau}\sin\left(\frac{\tau}{\varepsilon}\right)$ and $\frac{1}{\tau}\sin\left(\frac{\tau}{\varepsilon^2}\right)$ instead of $\frac{1}{\varepsilon}$ and $\frac{1}{\varepsilon^2}$ such that (2.11) is second order in terms of τ for any fixed $0 < \varepsilon \le 1$ and $\|\Phi^1\|_\infty := \max\limits_{0\le j\le M} |\Phi_j^1| \lesssim 1$ for $0 < \varepsilon \le 1$. We remark here that, when $\varepsilon = 1$, we can simply replace them by 1.

Among all the four FDTD methods, they are all time symmetric, the LFFD method (2.6) is completely explicit and its computational cost per step is $O(M)$. In fact, it might be the simplest and most efficient discretization for the NLDE when $\varepsilon = 1$ and thus it has been widely used in the literature when $\varepsilon = 1$ [20, 43, 60]. The SIFD1 method (2.7) is implicit, however at each time step for $n \ge 1$, the linear system is decoupled and so can be solved explicitly for $j = 0, 1, ..., M-1$

$$\begin{aligned} \Phi_j^{n+1} = &\left[(i - \tau V_j^n) I_2 - \frac{\tau}{\varepsilon^2}\sigma_3 + \tau A_{1,j}^n \sigma_1 - \tau \mathbf{F}_j^n \right]^{-1} \\ &\left[\left((i + \tau V_j^n) I_2 + \frac{\tau}{\varepsilon^2}\sigma_3 - \tau A_{1,j}^n \sigma_1 + \tau \mathbf{F}_j^n \right) \Phi_j^{n-1} - \frac{2i\tau}{\varepsilon} \sigma_1 \delta_x \Phi_j^n \right], \end{aligned} \tag{2.12}$$

and thus the computational cost per step is also $O(M)$.

The SIFD2 (2.8) is implicit, however at each time step for $n \ge 1$, the corresponding linear system is decoupled in phase (Fourier) space and can be solved explicitly in phase space for $l = -M/2, \ldots, M/2-1$ as

$$\widetilde{(\Phi^{n+1})}_l = \left(iI_2 - \frac{\tau \sin(\mu_l h)}{\varepsilon h}\sigma_1 - \frac{\tau}{\varepsilon^2}\sigma_3 \right)^{-1} \left[\left(iI_2 + \frac{\tau \sin(\mu_l h)}{\varepsilon h}\sigma_1 + \frac{\tau}{\varepsilon^2}\sigma_3 \right) \widetilde{(\Phi^{n-1})}_l + 2\tau \widetilde{\mathbf{G}(\Phi^n)}_l \right], \tag{2.13}$$

where $\mathbf{G}(\Phi^n) = (\mathbf{G}(\Phi^n)_0, \mathbf{G}(\Phi^n)_1, \ldots, \mathbf{G}(\Phi^n)_M)^T \in X_M$ with $\mathbf{G}(\Phi^n)_j = \left[V_j^n I_2 - A_{1,j}^n \sigma_1 + \mathbf{F}_j^n \right] \Phi_j^n$ for $j = 0, 1, \ldots, M$, and thus its computational cost per step is $O(M \ln M)$. The CNFD method (2.9) is implicit and at each time step for $n \ge 0$, we need to solve a nonlinear coupled system. It needs to be solved via a solver for nonlinear coupled system, and thus its computational cost per step depends on which nonlinear method to choose, and it is usually much larger than $O(M)$, especially in 2D and 3D. Based on the computational cost per time step, the LFFD method is the most efficient one and the CNFD method is the most expensive one.

Let $0 < T < T^*$ with T^* being the maximal existence time of the solution, and denote $\Omega_T = [0, T] \times \Omega$. We assume the electromagnetic potentials $V \in C(\overline{\Omega}_T)$ and $A_1 \in C(\overline{\Omega}_T)$ and denote

$$(A) \qquad V_{\max} := \max_{(t,x)\in\overline{\Omega}_T} |V(t,x)|, \qquad A_{1,\max} := \max_{(t,x)\in\overline{\Omega}_T} |A_1(t,x)|. \tag{2.14}$$

Similar to the linear stability analysis for the FDTD methods to the Dirac equation via the von Neumann method in [11], we can show that the CNFD method (2.9) is unconditionally stable, i.e. it is stable for any $\tau > 0$, $h > 0$ and $0 < \varepsilon \le 1$; the LFFD method (2.6), SIFD1 method (2.7) and SIFD2 method (2.8) are stable under the following stability conditions

$$\text{LFFD}: \quad 0 < \tau \le \frac{\varepsilon^2 h}{\varepsilon^2 h (V_{\max} + F_{\max}) + \sqrt{h^2 + \varepsilon^2 (1 + \varepsilon h A_{1,\max})^2}}, \tag{2.15}$$

$$\text{SIFD1}: \quad 0 < \tau \le \varepsilon h, \qquad h > 0, \qquad 0 < \varepsilon \le 1, \tag{2.16}$$

$$\text{SIFD2}: \quad 0 < \tau \le \frac{1}{V_{\max} + A_{1,\max} + F_{\max}}, \tag{2.17}$$

where $F_{\max} = (|\lambda_1| + |\lambda_2|) \max_{0\le j\le M, n\ge 0} |\Phi_j^n|^2$.

2.2. Mass and energy conservation

For the CNFD method (2.9), we have the following conservative properties.

Lemma 1. *The CNFD method* (2.9) *conserves the mass in the discretized level, i.e.*

$$\|\Phi^n\|_{l^2}^2 := h\sum_{j=0}^{M-1}|\Phi_j^n|^2 \equiv h\sum_{j=0}^{M-1}|\Phi_j^0|^2 = \|\Phi^0\|_{l^2}^2 = h\sum_{j=0}^{M-1}|\Phi_0(x_j)|^2, \qquad n\geq 0. \tag{2.18}$$

Furthermore, if $V(t,x)=V(x)$ and $A_1(t,x)=A_1(x)$ are time independent, the CNFD method (2.9) *conserves the energy as well,*

$$\begin{aligned} E_h^n &= h\sum_{j=0}^{M-1}\left[-\frac{i}{\varepsilon}(\Phi_j^n)^*\sigma_1\delta_x\Phi_j^n + \frac{1}{\varepsilon^2}(\Phi_j^n)^*\sigma_3\Phi_j^n + V(x_j)|\Phi_j^n|^2 - A_1(x_j)(\Phi_j^n)^*\sigma_1\Phi_j^n + G(\Phi_j^n)\right] \\ &\equiv E_h^0, \qquad n\geq 0, \end{aligned} \tag{2.19}$$

where $G(\Phi)$ is given in (1.20).

Proof: The proof of mass conservation (2.18) of the CNFD method is similar to the case of the Dirac equation in [11] and thus it is omitted here for brevity. In order to prove the energy conservation (2.19), multiplying both sides of (2.9) from left by $2h\,(\Phi_j^{n+1}-\Phi_j^n)^*$ and taking the real part, noticing (1.15) and (1.20), we have

$$\begin{aligned} &-h\,\mathrm{Re}\left[\frac{i}{\varepsilon}(\Phi_j^{n+1}-\Phi_j^n)^*\sigma_1\delta_x(\Phi_j^{n+1}+\Phi_j^n)\right] + \frac{h}{\varepsilon^2}\left[(\Phi_j^{n+1})^*\sigma_3\Phi_j^{n+1} - (\Phi_j^n)^*\sigma_3\Phi_j^n\right] + h\left[G(\Phi_j^{n+1}) - G(\Phi_j^n)\right] \\ &\quad + hV(x_j)(|\Phi_j^{n+1}|^2 - |\Phi_j^n|^2) - hA_1(x_j)\left[(\Phi_j^{n+1})^*\sigma_1\Phi_j^{n+1} - (\Phi_j^n)^*\sigma_1\Phi_j^n\right] = 0. \end{aligned} \tag{2.20}$$

Summing (2.20) for $j=0,1,\ldots,M-1$ and noticing the summation by parts formula

$$h\sum_{j=0}^{M-1}\mathrm{Re}\left(\frac{i}{\varepsilon}(\Phi_j^{n+1}-\Phi_j^n)^*\sigma_1\delta_x(\Phi_j^{n+1}+\Phi_j^n)\right) = \frac{ih}{\varepsilon}\sum_{j=0}^{M-1}(\Phi_j^{n+1})^*\sigma_1\delta_x\Phi_j^{n+1} - \frac{ih}{\varepsilon}\sum_{j=0}^{M-1}(\Phi_j^n)^*\sigma_1\delta_x\Phi_j^n,$$

we have

$$\begin{aligned} 0 =& -\frac{ih}{\varepsilon}\sum_{j=0}^{M-1}(\Phi_j^{n+1})^*\sigma_1\delta_x\Phi_j^{n+1} + \frac{h}{\varepsilon^2}\sum_{j=0}^{M-1}(\Phi_j^{n+1})^*\sigma_3\Phi_j^{n+1} + h\sum_{j=0}^{M-1}G(\Phi_j^{n+1}) \\ &+ h\sum_{j=0}^{M-1}\left[V(x_j)|\Phi_j^{n+1}|^2 - A_1(x_j)(\Phi_j^{n+1})^*\sigma_1\Phi_j^{n+1}\right] + \frac{ih}{\varepsilon}\sum_{j=0}^{M-1}(\Phi_j^n)^*\sigma_1\delta_x\Phi_j^n \\ &- \frac{h}{\varepsilon^2}\sum_{j=0}^{M-1}(\Phi_j^n)^*\sigma_3\Phi_j^n - h\sum_{j=0}^{M-1}G(\Phi_j^n) - h\sum_{j=0}^{M-1}\left[V(x_j)|\Phi_j^n|^2 - A_1(x_j)(\Phi_j^n)^*\sigma_1\Phi_j^n\right], \end{aligned}$$

which immediately implies (2.19). □

2.3. Error estimates

Motivated by the analytical results of the NLDE, we assume that the exact solution of (2.1) satisfies $\Phi\in C^3([0,T];(L^\infty(\Omega))^2)\cap C^2([0,T];(W_p^{1,\infty}(\Omega))^2)\cap C^1([0,T];(W_p^{2,\infty}(\Omega))^2)\cap C([0,T];(W_p^{3,\infty}(\Omega))^2)$ and

$$(B) \qquad \left\|\frac{\partial^{r+s}}{\partial t^r\partial x^s}\Phi\right\|_{L^\infty([0,T];(L^\infty(\Omega))^2)} \lesssim \frac{1}{\varepsilon^{2r}}, \quad 0\leq r\leq 3,\ 0\leq r+s\leq 3, \quad 0<\varepsilon\leq 1, \tag{2.21}$$

where $W_p^{m,\infty}(\Omega) = \{u \mid u \in W^{m,\infty}(\Omega),\ \partial_x^l u(a) = \partial_x^l u(b),\ l = 0, \ldots, m-1\}$ for $m \geq 1$ and here the boundary values are understood in the trace sense. In the subsequent discussion, we will omit Ω when referring to the space norm taken on Ω. We denote

$$M_0 := \max_{0 \leq t \leq T} \|\Phi(t,x)\|_{L^\infty} \lesssim 1. \tag{2.22}$$

Define the grid error function $\mathbf{e}^n = (\mathbf{e}_0^n, \mathbf{e}_1^n, \ldots, \mathbf{e}_M^n)^T \in X_M$ as:

$$\mathbf{e}_j^n = \Phi(t_n, x_j) - \Phi_j^n, \qquad j = 0, 1, \ldots, M, \quad n \geq 0, \tag{2.23}$$

with Φ_j^n being the approximations obtained from the FDTD methods.

For the CNFD (2.9), we can establish the error bound (see its proof in Appendix A).

Theorem 2.1. *Assume $0 < \tau \lesssim \varepsilon^3 h^{\frac{1}{4}}$, under the assumptions (A) and (B), there exist constants $h_0 > 0$ and $\tau_0 > 0$ sufficiently small and independent of ε, such that for any $0 < \varepsilon \leq 1$, when $0 < h \leq h_0$ and $0 < \tau \leq \tau_0$ satisfying $0 < h \lesssim \varepsilon^{\frac{2}{3}}$, we have the following error estimate for the CNFD method (2.9) with (2.10)*

$$\|\mathbf{e}^n\|_{l^2} \lesssim \frac{h^2}{\varepsilon} + \frac{\tau^2}{\varepsilon^6}, \qquad \|\Phi^n\|_{l^\infty} \leq 1 + M_0, \qquad 0 \leq n \leq \frac{T}{\tau}. \tag{2.24}$$

Similarly, for the LFFD (2.6), we can establish the error estimate (see its proof in Appendix B).

Theorem 2.2. *Assume $0 < \tau \lesssim \varepsilon^3 h^{\frac{1}{4}}$, under the assumptions (A) and (B), there exist constants $h_0 > 0$ and $\tau_0 > 0$ sufficiently small and independent of ε, such that for any $0 < \varepsilon \leq 1$, when $0 < h \leq h_0$ and $0 < \tau \leq \tau_0$ satisfying $0 < \tau \lesssim \min\{h, \varepsilon^2\}$, $0 < h \lesssim \varepsilon^{\frac{2}{3}}$ and the stability condition (2.15), we have the following error estimate for the LFFD (2.6) with (2.10) and (2.11)*

$$\|\mathbf{e}^n\|_{l^2} \lesssim \frac{h^2}{\varepsilon} + \frac{\tau^2}{\varepsilon^6}, \qquad \|\Phi^n\|_{l^\infty} \leq 1 + M_0, \qquad 0 \leq n \leq \frac{T}{\tau}. \tag{2.25}$$

For the SIFD1 and SIFD2, we have error estimates with the proof omitted for brevity.

Theorem 2.3. *Assume $0 < \tau \lesssim \varepsilon^3 h^{\frac{1}{4}}$, under the assumptions (A) and (B), there exist constants $h_0 > 0$ and $\tau_0 > 0$ sufficiently small and independent of ε, such that for any $0 < \varepsilon \leq 1$, when $0 < h \leq h_0$ and $0 < \tau \leq \tau_0$ satisfying $0 < \tau \lesssim h$, $0 < h \lesssim \varepsilon^{\frac{2}{3}}$ and the stability condition (2.16), we have the following error estimate for the SIFD1 (2.7) with (2.10) and (2.11)*

$$\|\mathbf{e}^n\|_{l^2} \lesssim \frac{h^2}{\varepsilon} + \frac{\tau^2}{\varepsilon^6}, \qquad \|\Phi^n\|_{l^\infty} \leq 1 + M_0, \qquad 0 \leq n \leq \frac{T}{\tau}.$$

Theorem 2.4. *Assume $0 < \tau \lesssim \varepsilon^3 h^{\frac{1}{4}}$, under the assumptions (A) and (B), there exist constants $h_0 > 0$ and $\tau_0 > 0$ sufficiently small and independent of ε, such that for any $0 < \varepsilon \leq 1$, when $0 < h \leq h_0$ and $0 < \tau \leq \tau_0$ satisfying $0 < h \lesssim \varepsilon^{\frac{2}{3}}$ and the stability condition (2.17), we have the following error estimate for the SIFD2 (2.8) with (2.10) and (2.11)*

$$\|\mathbf{e}^n\|_{l^2} \lesssim \frac{h^2}{\varepsilon} + \frac{\tau^2}{\varepsilon^6}, \qquad \|\Phi^n\|_{l^\infty} \leq 1 + M_0, \qquad 0 \leq n \leq \frac{T}{\tau}.$$

Based on Theorems 2.1-2.4, the four FDTD methods studied here share the same temporal/spatial resolution capacity in the nonrelativistic limit regime. In fact, given an accuracy bound $\delta_0 > 0$, the ε-scalability of the four FDTD methods is:

$$\tau = O\left(\varepsilon^3 \sqrt{\delta_0}\right) = O(\varepsilon^3), \qquad h = O\left(\sqrt{\delta_0 \varepsilon}\right) = O\left(\sqrt{\varepsilon}\right), \qquad 0 < \varepsilon \ll 1.$$

Remark 2.1. *The above Theorems are still valid in high dimensions provided that the conditions $0 < \tau \lesssim \varepsilon^3 h^{\frac{1}{4}}$ and $0 < h \lesssim \varepsilon^{\frac{2}{3}}$ are replaced by $0 < \tau \lesssim \varepsilon^3 h^{C_d}$ and $0 < h \lesssim \varepsilon^{\frac{1}{2(1-C_d)}}$, respectively, with $C_d = \frac{d}{4}$ for $d = 1, 2, 3$.*

3. An EWI-FP method and its analysis

In this section, we propose an EWI-FP method to solve the NLDE (2.1) and establish its error bound.

3.1. The EWI-FP method

Denote

$$Y_M = Z_M \times Z_M, \quad Z_M = \text{span}\left\{\phi_l(x) = e^{i\mu_l(x-a)},\ l = -\frac{M}{2}, -\frac{M}{2}+1, \ldots, \frac{M}{2}-1\right\}.$$

Let $[C_p(\overline{\Omega})]^2$ be the function space consisting of all periodic vector function $U(x):\ \overline{\Omega} = [a,b] \to \mathbb{C}^2$. For any $U(x) \in [C_p(\overline{\Omega})]^2$ and $U \in X_M$, define $P_M:\ [L^2(\Omega)]^2 \to Y_M$ as the standard projection operator [68], $I_M:\ [C_p(\overline{\Omega})]^2 \to Y_M$ and $I_M : X_M \to Y_M$ as the standard interpolation operator, i.e.

$$(P_M U)(x) = \sum_{l=-M/2}^{M/2-1} \widehat{U}_l\, e^{i\mu_l(x-a)}, \quad (I_M U)(x) = \sum_{l=-M/2}^{M/2-1} \widetilde{U}_l\, e^{i\mu_l(x-a)}, \qquad a \le x \le b,$$

with

$$\widehat{U}_l = \frac{1}{b-a}\int_a^b U(x)\, e^{-i\mu_l(x-a)}\, dx, \quad \widetilde{U}_l = \frac{1}{M}\sum_{j=0}^{M-1} U_j\, e^{-2ijl\pi/M}, \quad l = -\frac{M}{2}, \ldots, \frac{M}{2}-1, \tag{3.1}$$

where $U_j = U(x_j)$ when U is a function.

The Fourier spectral discretization for the NLDE (2.1) is as follows:
Find $\Phi_M := \Phi_M(t,x) \in Y_M$, i.e.

$$\Phi_M(t,x) = \sum_{l=-M/2}^{M/2-1} \widehat{(\Phi_M)_l}(t)\, e^{i\mu_l(x-a)}, \qquad a \le x \le b, \qquad t \ge 0, \tag{3.2}$$

such that for $a < x < b$ and $t > 0$,

$$i\partial_t \Phi_M = \left[-\frac{i}{\varepsilon}\sigma_1\partial_x + \frac{1}{\varepsilon^2}\sigma_3\right]\Phi_M + P_M\left[\left(V(t,x)I_2 - A_1(t,x)\sigma_1 + \mathbf{F}(\Phi_M)\right)\Phi_M\right]. \tag{3.3}$$

Substituting (3.2) into (3.3), noticing the orthogonality of $\phi_l(x)$, we get for $l = -\frac{M}{2}, -\frac{M}{2}+1, \ldots, \frac{M}{2}-1$,

$$i\,\frac{d}{dt}\widehat{(\Phi_M)_l}(t) = \left[\frac{\mu_l}{\varepsilon}\sigma_1 + \frac{1}{\varepsilon^2}\sigma_3\right]\widehat{(\Phi_M)_l}(t) + \widehat{\mathbf{G}(\Phi_M)_l}(t), \qquad t > 0, \tag{3.4}$$

where

$$\mathbf{G}(\Phi_M) = \left(V(t,x)I_2 - A_1(t,x)\sigma_1 + \mathbf{F}(\Phi_M)\right)\Phi_M, \qquad x \in \Omega, \quad t \ge 0. \tag{3.5}$$

For $t \ge 0$ and each l ($l = -\frac{M}{2}, -\frac{M}{2}+1, \ldots, \frac{M}{2}-1$), when t is near $t = t_n$ ($n \ge 0$), we rewrite the above ODEs as

$$i\,\frac{d}{ds}\widehat{(\Phi_M)_l}(t_n+s) = \frac{1}{\varepsilon^2}\Gamma_l\,\widehat{(\Phi_M)_l}(t_n+s) + \widehat{\mathbf{G}(\Phi_M)}_l^n(s), \qquad s > 0, \tag{3.6}$$

where $\Gamma_l = \mu_l\varepsilon\sigma_1 + \sigma_3 = Q_l\, D_l\, (Q_l)^*$ with $\delta_l = \sqrt{1+\varepsilon^2\mu_l^2}$ and

$$\Gamma_l = \begin{pmatrix} 1 & \mu_l\varepsilon \\ \mu_l\varepsilon & -1 \end{pmatrix}, \quad Q_l = \begin{pmatrix} \frac{1+\delta_l}{\sqrt{2\delta_l(1+\delta_l)}} & -\frac{\varepsilon\mu_l}{\sqrt{2\delta_l(1+\delta_l)}} \\ \frac{\varepsilon\mu_l}{\sqrt{2\delta_l(1+\delta_l)}} & \frac{1+\delta_l}{\sqrt{2\delta_l(1+\delta_l)}} \end{pmatrix}, \quad D_l = \begin{pmatrix} \delta_l & 0 \\ 0 & -\delta_l \end{pmatrix}, \tag{3.7}$$

and

$$\widehat{\mathbf{G}(\Phi_M)}_l^n(s) = \widehat{\mathbf{G}(\Phi_M)}_l(t_n+s), \qquad s \ge 0, \quad n \ge 0, \tag{3.8}$$

Solving the above ODE (3.6) via the integrating factor method, we obtain

$$\widehat{(\Phi_M)}_l(t_n+s) = e^{-is\Gamma_l/\varepsilon^2}\widehat{(\Phi_M)}_l(t_n) - i\int_0^s e^{i(w-s)\Gamma_l/\varepsilon^2}\widehat{\mathbf{G}(\Phi_M)}_l^n(w)\,dw, \qquad s\geq 0. \tag{3.9}$$

Taking $s=\tau$ in (3.9) we have

$$\widehat{(\Phi_M)}_l(t_{n+1}) = e^{-i\tau\Gamma_l/\varepsilon^2}\widehat{(\Phi_M)}_l(t_n) - i\int_0^\tau e^{\frac{i(w-\tau)}{\varepsilon^2}\Gamma_l}\widehat{\mathbf{G}(\Phi_M)}_l^n(w)dw. \tag{3.10}$$

To obtain a numerical method with second order accuracy in time, we approximate the integral in (3.10) via the Gautschi-type rule, which has been widely used for integrating highly oscillatory ODEs [13, 37, 42], as

$$\int_0^\tau e^{\frac{i(w-\tau)}{\varepsilon^2}\Gamma_l}\widehat{\mathbf{G}(\Phi_M)}_l^0(w)\,dw \approx \int_0^\tau e^{\frac{i(w-\tau)}{\varepsilon^2}\Gamma_l}\,dw\,\widehat{\mathbf{G}(\Phi_M)}_l^0(0) = -i\varepsilon^2\Gamma_l^{-1}\left[I_2 - e^{-\frac{i\tau}{\varepsilon^2}\Gamma_l}\right]\widehat{\mathbf{G}(\Phi_M)}_l^0(0), \tag{3.11}$$

and for $n\geq 1$

$$\begin{aligned}\int_0^\tau e^{\frac{i(w-\tau)}{\varepsilon^2}\Gamma_l}\widehat{\mathbf{G}(\Phi_M)}_l^n(w) &\approx \int_0^\tau e^{\frac{i(w-\tau)}{\varepsilon^2}\Gamma_l}\left(\widehat{\mathbf{G}(\Phi_M)}_l^n(0) + w\,\delta_t^-\widehat{\mathbf{G}(\Phi_M)}_l^n(0)\right)dw\\ &= -i\varepsilon^2\Gamma_l^{-1}\left[I_2 - e^{-\frac{i\tau}{\varepsilon^2}\Gamma_l}\right]\widehat{\mathbf{G}(\Phi_M)}_l^n(0) + \left[-i\varepsilon^2\tau\Gamma_l^{-1} + \varepsilon^4\Gamma_l^{-2}\left(I_2 - e^{-\frac{i\tau}{\varepsilon^2}\Gamma_l}\right)\right]\delta_t^-\widehat{\mathbf{G}(\Phi_M)}_l^n(0),\end{aligned} \tag{3.12}$$

where we have approximated the time derivative $\partial_t\widehat{\mathbf{G}(\Phi_M)}_l^n(s)$ at $s=0$ by finite difference as

$$\partial_t\widehat{\mathbf{G}(\Phi_M)}_l^n(0) \approx \delta_t^-\widehat{\mathbf{G}(\Phi_M)}_l^n(0) = \frac{1}{\tau}\left[\widehat{\mathbf{G}(\Phi_M)}_l^n(0) - \widehat{\mathbf{G}(\Phi_M)}_l^{n-1}(0)\right]. \tag{3.13}$$

Now, we are ready to describe our scheme. Let $\Phi_M^n(x)$ be the approximation of $\Phi_M(t_n,x)$ $(n\geq 0)$. Choosing $\Phi_M^0(x) = (P_M\Phi_0)(x)$, an *exponential wave integrator Fourier spectral* (EWI-FS) discretization for the NLDE (2.1) is to update the numerical approximation $\Phi_M^{n+1}(x)\in Y_M$ $(n=0,1,\ldots)$ as

$$\Phi_M^{n+1}(x) = \sum_{l=-M/2}^{M/2-1}(\widehat{\Phi_M^{n+1}})_l\,e^{i\mu_l(x-a)}, \qquad a\leq x\leq b, \qquad n\geq 0, \tag{3.14}$$

where for $l=-\frac{M}{2},..,\frac{M}{2}-1$,

$$(\widehat{\Phi_M^{n+1}})_l = \begin{cases} e^{-i\tau\Gamma_l/\varepsilon^2}\widehat{(\Phi_M^0)}_l - \varepsilon^2\Gamma_l^{-1}\left[I_2 - e^{-\frac{i\tau}{\varepsilon^2}\Gamma_l}\right]\widehat{\mathbf{G}(\Phi_M^0)}_l, & n=0,\\ e^{-i\tau\Gamma_l/\varepsilon^2}\widehat{(\Phi_M^n)}_l - iQ_l^{(1)}(\tau)\,\widehat{\mathbf{G}(\Phi_M^n)}_l - iQ_l^{(2)}(\tau)\delta_t^-\widehat{\mathbf{G}(\Phi_M^n)}_l, & n\geq 1,\end{cases} \tag{3.15}$$

with the matrices $Q_l^{(1)}(\tau)$ and $Q_l^{(2)}(\tau)$ given as

$$Q_l^{(1)}(\tau) = -i\varepsilon^2\Gamma_l^{-1}\left[I_2 - e^{-\frac{i\tau}{\varepsilon^2}\Gamma_l}\right], \quad Q_l^{(2)}(\tau) = -i\varepsilon^2\tau\Gamma_l^{-1} + \varepsilon^4\Gamma_l^{-2}\left(I_2 - e^{-\frac{i\tau}{\varepsilon^2}\Gamma_l}\right), \tag{3.16}$$

and

$$\mathbf{G}(\Phi_M^n) = (V(t_n,x)I_2 - A_1(t_n,x)\sigma_1 + \mathbf{F}(\Phi_M^n))\,\Phi_M^n, \qquad n\geq 0. \tag{3.17}$$

The above procedure is not suitable in practice due to the difficulty in computing the Fourier coefficients through integrals in (3.1). Here we present an efficient implementation by choosing $\Phi_M^0(x)$ as the interpolant of $\Phi_0(x)$ on the grids $\{x_j, j=0,1,\ldots,M\}$ and approximate the integrals in (3.1) by a quadrature rule.

Let Φ_j^n be the numerical approximation of $\Phi(t_n,x_j)$ for $j=0,1,2,\ldots,M$ and $n\geq 0$, and denote $\Phi^n\in X_M$ as the vector with components Φ_j^n. Choosing $\Phi_j^0 = \Phi_0(x_j)$ $(j=0,1,\ldots,M)$, an *EWI Fourier pseudospectral* (EWI-FP) method for computing Φ^{n+1} for $n\geq 0$ reads

$$\Phi_j^{n+1} = \sum_{l=-M/2}^{M/2-1}\widetilde{(\Phi^{n+1})}_l e^{2ijl\pi/M}, \quad j=0,1,...,M, \tag{3.18}$$

where

$$\widetilde{(\Phi^{n+1})}_l = \begin{cases} e^{-i\tau\Gamma_l/\varepsilon^2}\widetilde{(\Phi^0)}_l - \varepsilon^2\Gamma_l^{-1}\left[I_2 - e^{-\frac{i\tau}{\varepsilon^2}\Gamma_l}\right]\widetilde{\mathbf{G}(\Phi^0)}_l, & n=0, \\ e^{-i\tau\Gamma_l/\varepsilon^2}\widetilde{(\Phi^n)}_l - iQ_l^{(1)}(\tau)\,\widetilde{\mathbf{G}(\Phi^n)}_l - iQ_l^{(2)}(\tau)\delta_t^-\widetilde{\mathbf{G}(\Phi^n)}_l, & n\geq 1. \end{cases} \tag{3.19}$$

The EWI-FP (3.18)-(3.19) is explicit, and can be solved efficiently by the fast Fourier transform (FFT). The memory cost is $O(M)$ and the computational cost per time step is $O(M\log M)$.

Similar to the analysis of the EWI-FP method for the Dirac equation in [11], we can obtain that the EWI-FP for the NLDE is stable under the stability condition (details are omitted here for brevity)

$$0<\tau\lesssim 1, \quad 0<\varepsilon\leq 1. \tag{3.20}$$

3.2. Error estimates

In order to obtain an error estimate for the EWI methods (3.14)-(3.15) and (3.18)-(3.19), motivated by the results in [35, 58], we assume that there exists an integer $m_0\geq 2$ such that the exact solution $\Phi(t,x)$ of the NLDE (2.1) satisfies

$$(C) \qquad \|\Phi\|_{L^\infty([0,T];(H_p^{m_0})^2)}\lesssim 1, \quad \|\partial_t\Phi\|_{L^\infty([0,T];(L^2)^2)}\lesssim\frac{1}{\varepsilon^2}, \quad \|\partial_{tt}\Phi\|_{L^\infty([0,T];(L^2)^2)}\lesssim\frac{1}{\varepsilon^4},$$

where $H_p^k(\Omega)=\{u\mid u\in H^k(\Omega),\ \partial_x^l u(a)=\partial_x^l u(b),\ l=0,\ldots,k-1\}$. In addition, we assume electromagnetic potentials satisfy

$$(D) \qquad \|V\|_{W^{2,\infty}([0,T];L^\infty)}+\|A_1\|_{W^{2,\infty}([0,T];L^\infty)}\lesssim 1.$$

We can establish the following error estimate for the EWI-FS method (see its proof in Appendix C).

Theorem 3.1. *Let $\Phi_M^n(x)$ be the approximation obtained from the EWI-FS (3.14)-(3.15). Assume $0<\tau\lesssim\varepsilon^2h^{1/4}$, under the assumptions (C) and (D), there exists $h_0>0$ and $\tau_0>0$ sufficiently small and independent of ε such that, for any $0<\varepsilon\leq 1$, when $0<h\leq h_0$ and $0<\tau\leq\tau_0$, we have the error estimate*

$$\|\Phi(t_n,x)-\Phi_M^n(x)\|_{L^2}\lesssim\frac{\tau^2}{\varepsilon^4}+h^{m_0}, \qquad \|\Phi_M^n(x)\|_{L^\infty}\leq 1+M_0, \qquad 0\leq n\leq\frac{T}{\tau}. \tag{3.21}$$

Remark 3.1. *The same error estimate in Theorem 3.1 holds for the EWI-FP (3.18)-(3.19) and the proof is quite similar to that of Theorem 3.1. In addition, the above Theorem is still valid in high dimensions provided that the condition $0<\tau\lesssim\varepsilon^2h^{\frac{1}{4}}$ is replaced by $0<\tau\lesssim\varepsilon^2h^{C_d}$.*

From this theorem, the temporal/spatial resolution capacity of the EWI-FP method for the NLDE in the nonrelativistic limit regime is: $h=O(1)$ and $\tau=O(\varepsilon^2)$. In fact, for a given accuracy bound $\delta_0>0$, the ε-scalability of the EWI-FP is:

$$\tau=O\left(\varepsilon^2\sqrt{\delta_0}\right)=O(\varepsilon^2), \qquad h=O\left(\delta_0^{1/m_0}\right)=O\left(1\right), \qquad 0<\varepsilon\ll 1.$$

Similar to the Appendix D in [11] for the Dirac equation, it is straightforward to generalize the EWI-FP to the NLDE (1.14) in 2D and (1.4) in 1D, 2D and 3D and the details are omitted here for brevity.

4. A TSFP method and its analysis

In this section, we present a time-splitting Fourier pseudospectral (TSFP) method for the NLDE (2.1). From time $t=t_n$ to time $t=t_{n+1}$, the NLDE (2.1) is split into two steps. One solves first

$$i\partial_t\Phi(t,x)=\left[-\frac{i}{\varepsilon}\sigma_1\partial_x+\frac{1}{\varepsilon^2}\sigma_3\right]\Phi(t,x), \quad x\in\Omega, \tag{4.1}$$

with the periodic boundary condition (2.2) for the time step of length τ, followed by solving

$$i\partial_t \Phi(t,x) = [V(t,x)I_2 - A_1(t,x)\sigma_1 + \mathbf{F}(\Phi(t,x))]\,\Phi(t,x), \quad x \in \Omega, \tag{4.2}$$

for the same time step. Eq. (4.1) will be first discretized in space by the Fourier spectral method and then integrated (in phase or Fourier space) in time *exactly* [11, 16]. For the ODEs (4.2), multiplying $\Phi^*(t,x)$ from the left, we get

$$i\Phi^*(t,x)\partial_t \Phi(t,x) = \Phi^*(t,x)\,[V(t,x)I_2 - A_1(t,x)\sigma_1 + \mathbf{F}(\Phi(t,x))]\,\Phi(t,x), \quad x \in \Omega. \tag{4.3}$$

Taking conjugate to both sides of the above equation, noticing (1.15), we obtain

$$-i\partial_t \Phi^*(t,x)\,\Phi(t,x) = \Phi^*(t,x)\,[V(t,x)I_2 - A_1(t,x)\sigma_1^* + \mathbf{F}(\Phi(t,x))]\,\Phi(t,x), \quad x \in \Omega, \tag{4.4}$$

where $\sigma_1^* = \overline{\sigma_1}^T$. Subtracting (4.4) from (4.3), noticing (1.15), $\sigma_1^* = \sigma_1$ and $\sigma_3^* = \sigma_3$, we obtain for $\rho(t,x) = |\Phi(t,x)|^2$

$$\partial_t \rho(t,x) = 0, \qquad t_n \le t \le t_{n+1}, \qquad x \in \Omega, \tag{4.5}$$

which immediately implies $\rho(t,x) = \rho(t_n,x)$.

If $A_1(t,x) \equiv 0$, multiplying (4.2) from the left by $\Phi^*(t,x)\sigma_3$ and by a similar procedure, we get $\Phi^*(t,x)\sigma_3\Phi(t,x) = \Phi^*(t_n,x)\sigma_3\Phi(t_n,x)$ for $t_n \le t \le t_{n+1}$ and $x \in \Omega$. Thus if $\lambda_1 = 0$ or $A_1(t,x) \equiv 0$, we have

$$\mathbf{F}(\Phi(t,x)) = \mathbf{F}(\Phi(t_n,x)), \qquad t_n \le t \le t_{n+1}, \qquad x \in \Omega. \tag{4.6}$$

Plugging (4.6) into (4.2), we obtain

$$i\partial_t \Phi(t,x) = [V(t,x)I_2 - A_1(t,x)\sigma_1 + \mathbf{F}(\Phi(t_n,x))]\,\Phi(t,x), \quad x \in \Omega, \tag{4.7}$$

which can be integrated *analytically* in time as

$$\Phi(t,x) = e^{-i\int_{t_n}^t [V(s,x)I_2 - A_1(s,x)\sigma_1 + \mathbf{F}(\Phi(t_n,x))]ds}\,\Phi(t_n,x), \qquad a \le x \le b, \quad t_n \le t \le t_{n+1}. \tag{4.8}$$

In practical computation, if $\lambda_1 = 0$ or $A_1(t,x) \equiv 0$, from time $t = t_n$ to $t = t_{n+1}$, we often combine the splitting steps via the Strang splitting [70] – which results in a second order TSFP method as

$$\begin{aligned}
\Phi_j^{(1)} &= \sum_{l=-M/2}^{M/2-1} e^{-i\tau\Gamma_l/2\varepsilon^2}\,\widetilde{(\Phi^n)}_l\, e^{i\mu_l(x_j-a)} = \sum_{l=-M/2}^{M/2-1} Q_l\, e^{-i\tau D_l/2\varepsilon^2}\,(Q_l)^*\,\widetilde{(\Phi^n)}_l\, e^{\frac{2ijl\pi}{M}},\\
\Phi_j^{(2)} &= e^{-i\int_{t_n}^{t_{n+1}} \mathbf{W}(t,x_j)\,dt}\,\Phi_j^{(1)} = P_j\, e^{-i\,\Lambda_j}\,P_j^*\,\Phi_j^{(1)}, \qquad j = 0,1,\ldots,M, \qquad n \ge 0,\\
\Phi_j^{n+1} &= \sum_{l=-M/2}^{M/2-1} e^{-i\tau\Gamma_l/2\varepsilon^2}\,\widetilde{(\Phi^{(2)})}_l\, e^{i\mu_l(x_j-a)} = \sum_{l=-M/2}^{M/2-1} Q_l\, e^{-i\tau D_l/2\varepsilon^2}\,(Q_l)^*\,\widetilde{(\Phi^{(2)})}_l\, e^{\frac{2ijl\pi}{M}},
\end{aligned} \tag{4.9}$$

where $\int_{t_n}^{t_{n+1}} \mathbf{W}(t,x_j)dt = V_j^{(1)}\,I_2 - A_{1,j}^{(1)}\,\sigma_1 + \tau\mathbf{F}(\Phi_j^{(1)}) = \left(V_j^{(1)} + \tau\lambda_2|\Phi_j^{(1)}|^2\right) I_2 - A_{1,j}^{(1)}\,\sigma_1 + \tau\lambda_1\,(\Phi_j^{(1)})^*\sigma_3\Phi_j^{(1)}\sigma_3$ $= P_j\,\Lambda_j\,P_j^*$ with $V_j^{(1)} = \int_{t_n}^{t_{n+1}} V(t,x_j)dt$, $A_{1,j}^{(1)} = \int_{t_n}^{t_{n+1}} A_1(t,x_j)dt$, $\Lambda_j = \mathrm{diag}(\Lambda_{j,+},\Lambda_{j,-})$, and $\Lambda_{j,\pm} = V_j^{(1)} + \tau\lambda_2|\Phi_j^{(1)}|^2 \pm \tau\lambda_1(\Phi_j^{(1)})^*\sigma_3\Phi_j^{(1)}$ and $P_j = I_2$ if $A_{1,j}^{(1)} = 0$, and resp., $\Lambda_{j,\pm} = V_j^{(1)} + \tau\lambda_2|\Phi_j^{(1)}|^2 \pm A_{1,j}^{(1)}$ and

$$P_j = P^{(0)} := \begin{pmatrix} \frac{1}{\sqrt{2}} & \frac{1}{\sqrt{2}} \\ -\frac{1}{\sqrt{2}} & \frac{1}{\sqrt{2}} \end{pmatrix}, \tag{4.10}$$

if $A_{1,j}^{(1)} \neq 0$ and $\lambda_1 = 0$.

Of course, if $\lambda_1 \neq 0$ and $A_1(t,x) \neq 0$, then $\Phi^*(t,x)\sigma_3\Phi(t,x)$ is no longer time-independent in the second step (4.2) due to that $\sigma_1^*\sigma_3^* = \sigma_1\sigma_3 \neq \sigma_3\sigma_1$. In this situation, we will spit (4.2) into two steps as: one first solves

$$i\partial_t\Phi(t,x) = [V(t,x)I_2 - A_1(t,x)\sigma_1]\,\Phi(t,x), \quad x \in \Omega, \tag{4.11}$$

followed by solving

$$i\partial_t\Phi(t,x) = \mathbf{F}(\Phi(t,x))\,\Phi(t,x), \quad x \in \Omega. \tag{4.12}$$

Similar to the Dirac equation [11], Eq. (4.11) can be integrated *analytically* in time. For Eq. (4.12), both $\rho(t,x)$ and $\Phi^*(t,x)\sigma_3\Phi(t,x)$ are invariant in time, i.e. $\rho(t,x) \equiv \rho(t_n,x)$ and $\Phi^*(t,x)\sigma_3\Phi(t,x) \equiv \Phi^*(t_n,x)\sigma_3\Phi(t_n,x)$ for $t_n \le t \le t_{n+1}$ and $x \in \bar{\Omega}$. Thus it collapses to

$$i\partial_t\Phi(t,x) = \mathbf{F}(\Phi(t_n,x))\,\Phi(t,x), \quad x \in \Omega, \tag{4.13}$$

and it can integrated *analytically* in time too. Similarly, a second-order TSFP method can be designed provided that we replace $\Phi^{(2)}$ in the third step by $\Phi^{(4)}$ and the second step in (4.9) by

$$\begin{aligned}
\Phi_j^{(2)} &= e^{-\frac{i}{2}\int_{t_n}^{t_{n+1}}\mathbf{F}(\Phi(t_n,x_j))\,dt}\,\Phi_j^{(1)} = e^{-i\,\Lambda_j^{(1)}}\,\Phi_j^{(1)},\\
\Phi_j^{(3)} &= e^{-i\int_{t_n}^{t_{n+1}}[V(t,x_j)I_2 - A_1(t,x_j)\sigma_1]\,dt}\,\Phi_j^{(2)} = P_j\,e^{-i\,\Lambda_j^{(2)}}\,P_j^*\,\Phi_j^{(2)},\\
\Phi_j^{(4)} &= e^{-\frac{i}{2}\int_{t_n}^{t_{n+1}}\mathbf{F}(\Phi(t_n,x_j))\,dt}\,\Phi_j^{(3)} = e^{-i\,\Lambda_j^{(1)}}\,\Phi_j^{(3)}, \qquad j = 0,1,\ldots,M, \qquad n \ge 0,
\end{aligned} \tag{4.14}$$

where $\Lambda_j^{(1)} = \mathrm{diag}(\Lambda_{j,+}^{(1)}, \Lambda_{j,-}^{(1)})$ with $\Lambda_{j,\pm}^{(1)} = \frac{\tau}{2}\left[\lambda_2|\Phi_j^{(1)}|^2 \pm \lambda_1(\Phi_j^{(1)})^*\sigma_3\Phi_j^{(1)}\right]$, $\Lambda_j^{(2)} = \mathrm{diag}(\Lambda_{j,+}^{(2)}, \Lambda_{j,-}^{(2)})$ with $\Lambda_{j,\pm}^{(2)} = V_j^{(1)} \pm A_{1,j}^{(1)}$, and $P_j = I_2$ if $A_{1,j}^{(1)} = 0$, and resp., $P_j = P^{(0)}$ if $A_{1,j}^{(1)} \neq 0$ for $j = 0,1,\ldots,M$.

Remark 4.1. *If the above definite integrals cannot be evaluated analytically, we can evaluate them numerically via the Simpson's quadrature rule as*

$$\begin{aligned}
V_j^{(1)} &= \int_{t_n}^{t_{n+1}} V(t,x_j)\,dt \approx \frac{\tau}{6}\left[V(t_n,x_j) + 4V\left(t_n+\frac{\tau}{2},x_j\right) + V(t_{n+1},x_j)\right],\\
A_{1,j}^{(1)} &= \int_{t_n}^{t_{n+1}} A_1(t,x_j)\,dt \approx \frac{\tau}{6}\left[A_1(t_n,x_j) + 4A_1\left(t_n+\frac{\tau}{2},x_j\right) + A_1(t_{n+1},x_j)\right].
\end{aligned}$$

Similar to the TSFP for the Dirac equation in [11], we can show that the TSFP (4.9) for the NLDE conserves the mass in the discretized level with the details omitted here for brevity.

Lemma 2. *The TSFP (4.9) conserves the mass in the discretized level, i.e.*

$$\|\Phi^n\|_{l^2}^2 := h\sum_{j=0}^{M-1}|\Phi_j^n|^2 \equiv h\sum_{j=0}^{M-1}|\Phi_j^0|^2 = \|\Phi^0\|_{l^2}^2 = h\sum_{j=0}^{M-1}|\Phi_0(x_j)|^2, \qquad n \ge 0. \tag{4.15}$$

From Lemma 2, we conclude that TSFP (4.9) is unconditionally stable. In addition, following the error estimate of the TSFP method for the nonlinear Schrödinger equation via the formal Lie calculus introduced in [53, 8], it is easy to show the following error estimate of the TSFP for the NLDE.

Lemma 3. *Let Φ^n be the approximation obtained from the TSFP (4.9). Assume $0 < \tau \lesssim \varepsilon^2 h^{1/4}$, under the assumptions (C) and (D), there exists $h_0 > 0$ and $\tau_0 > 0$ sufficiently small and independent of ε such that, for any $0 < \varepsilon \le 1$, when $0 < h \le h_0$ and $0 < \tau \le \tau_0$, we have the error estimate*

$$\|\Phi(t_n,x) - (I_M\Phi^n)(x)\|_{L^2} \lesssim \frac{\tau^2}{\varepsilon^4} + h^{m_0}, \qquad \|\Phi^n\|_{l^\infty} \le 1 + M_0, \qquad 0 \le n \le \frac{T}{\tau}. \tag{4.16}$$

Table 5.1: Spatial and temporal error analysis of the LFFD method for the NLDE (1.14).

Spatial Errors	$h_0 = 1/8$	$h_0/2$	$h_0/2^2$	$h_0/2^3$	$h_0/2^4$
$\varepsilon_0 = 1$	8.15E-2	2.02E-2	5.00E-3	1.25E-3	3.12E-4
order	-	2.01	2.01	2.00	2.00
$\varepsilon_0/2$	9.29E-2	2.30E-2	5.73E-3	1.43E-3	3.58E-4
order	-	2.01	2.01	2.00	2.00
$\varepsilon_0/2^2$	9.91E-2	2.46E-2	6.12E-3	1.53E-3	3.82E-4
order	-	2.01	2.01	2.00	2.00
$\varepsilon_0/2^3$	9.89E-2	2.47E-2	6.17E-3	1.54E-3	3.85E-4
order	-	2.00	2.00	2.00	2.00
$\varepsilon_0/2^4$	9.87E-2	2.48E-2	6.18E-3	1.54E-3	3.83E-4
order	-	1.99	2.00	2.00	2.01
Temporal Errors	$\tau_0 = 0.1$ $h_0 = 1/8$	$\tau_0/8$ $h_0/8\delta_1(\varepsilon)$	$\tau_0/8^2$ $h_0/8^2\delta_2(\varepsilon)$	$\tau_0/8^3$ $h_0/8^3\delta_3(\varepsilon)$	$\tau_0/8^4$ $h_0/8^4\delta_4(\varepsilon)$
$\varepsilon_0 = 1$	1.95E-1	2.67E-3	4.16E-5	6.50E-7	1.00E-8
order	-	2.06	2.00	2.00	2.01
$\varepsilon_0/2$	unstable	2.03E-2	3.14E-4	4.91E-6	7.67E-8
order	-	-	2.00	2.00	2.00
$\varepsilon_0/2^2$	unstable	4.65E-1	7.17E-3	1.11E-4	1.74E-6
order	-	-	2.01	2.00	2.00
$\varepsilon_0/2^3$	unstable	unstable	4.13E-1	6.08E-3	1.01E-4
order	-	-	-	2.03	1.97
$\varepsilon_0/2^4$	unstable	unstable	3.48	4.04E-1	6.20E-3
order	-	-	-	1.04	2.01

From Lemma 3, we can find the temporal/spatial resolution capacity of the TSFP method for the NLDE in the nonrelativistic limit regime, which is: $h = O(1)$ and $\tau = O(\varepsilon^2)$. In fact, for a given accuracy bound $\delta_0 > 0$, the ε-scalability of the TSFP is:

$$\tau = O\left(\varepsilon^2\sqrt{\delta_0}\right) = O(\varepsilon^2), \qquad h = O\left(\delta_0^{1/m_0}\right) = O\left(1\right), \qquad 0 < \varepsilon \ll 1. \tag{4.17}$$

Similar to the Appendix D in [11] for the Dirac equation, it is straightforward to generalize the TSFP to the NLDE (1.14) in 2D and (1.4) in 1D, 2D and 3D and the details are omitted here for brevity.

5. Numerical comparisons

In this section, we compare the accuracy of different numerical methods including the FDTD, EWI-FP and TSFP methods in solving the NLDE (1.14) in terms of the mesh size h, time step τ and the parameter $0 < \varepsilon \leq 1$. We will pay particular attention to the ε-scalability of different methods in the nonrelativistic limit regime, i.e. $0 < \varepsilon \ll 1$.

To test the accuracy, we take $d = 1$ and choose the electromagnetic potentials in the NLDE (1.14) as

$$A_1(t,x) = \frac{(x+1)^2}{1+x^2}, \qquad V(t,x) = \frac{1-x}{1+x^2}, \qquad x \in \mathbb{R}, \quad t \geq 0,$$

and the initial value as

$$\phi_1(0,x) = e^{-x^2/2}, \quad \phi_2(0,x) = e^{-(x-1)^2/2}, \qquad x \in \mathbb{R}.$$

The problem is solved numerically on an interval $\Omega = (-16, 16)$, i.e. $a = -16$ and $b = 16$, with periodic boundary conditions on $\partial\Omega$. The 'exact' solution $\Phi(t,x) = (\phi_1(t,x), \phi_2(t,x))^T$ is obtained numerically by

Table 5.2: Spatial and temporal error analysis of the SIFD1 method for the NLDE (1.14).

Spatial Errors	$h_0 = 1/8$	$h_0/2$	$h_0/2^2$	$h_0/2^3$	$h_0/2^4$
$\varepsilon_0 = 1$	8.15E-2	2.02E-2	5.00E-3	1.25E-3	3.12E-4
order	-	2.01	2.01	2.00	2.00
$\varepsilon_0/2$	9.29E-2	2.30E-2	5.73E-3	1.43E-3	3.58E-4
order	-	2.01	2.01	2.00	2.00
$\varepsilon_0/2^2$	9.91E-2	2.46E-2	6.12E-3	1.53E-3	3.82E-4
order	-	2.01	2.01	2.00	2.00
$\varepsilon_0/2^3$	9.89E-2	2.47E-2	6.17E-3	1.54E-3	3.85E-4
order	-	2.00	2.00	2.00	2.00
$\varepsilon_0/2^4$	9.87E-2	2.48E-2	6.18E-3	1.54E-3	3.83E-4
order	-	1.99	2.00	2.00	2.01
Temporal Errors	$\tau_0 = 0.1$ $h_0 = 1/8$	$\tau_0/8$ $h_0/8\delta_1(\varepsilon)$	$\tau_0/8^2$ $h_0/8^2\delta_2(\varepsilon)$	$\tau_0/8^3$ $h_0/8^3\delta_3(\varepsilon)$	$\tau_0/8^4$ $h_0/8^4\delta_4(\varepsilon)$
$\varepsilon_0 = 1$	1.69E-1	2.16E-3	4.08E-5	6.38E-7	9.81E-9
order	-	2.10	1.91	2.00	2.01
$\varepsilon_0/2$	unstable	3.23E-2	5.04E-4	7.87E-6	1.23E-7
order	-	-	2.00	2.00	2.00
$\varepsilon_0/2^2$	unstable	8.22E-1	1.62E-2	2.05E-4	3.20E-6
order	-	-	1.89	2.10	2.00
$\varepsilon_0/2^3$	unstable	unstable	8.00E-1	1.32E-2	1.97E-4
order	-	-	-	1.97	2.02
$\varepsilon_0/2^4$	unstable	unstable	4.44E-1	7.97E-1	1.27E-2
order	-	-	-	-0.28	2.00

using the TSFP method with a very fine mesh size and a small time step, e.g. $h_e = 1/16$ and $\tau_e = 10^{-7}$ for comparing with the numerical solutions obtained by EWI-FP and TSFP, and respectively $h_e = 1/4096$ for comparing with the numerical solutions obtained by FDTD methods. Denote $\Phi^n_{h,\tau}$ as the numerical solution obtained by a numerical method with mesh size h and time step τ. In order to quantify the convergence, we introduce

$$e_{h,\tau}(t_n) = \|\Phi^n - \Phi(t_n,\cdot)\|_{l^2} = \sqrt{h\sum_{j=0}^{M-1}|\Phi^n_j - \Phi(t_n,x_j)|^2}.$$

Table 5.1 lists spatial errors $e_{h,\tau_e}(t=2)$ with different h (upper part) and temporal errors $e_{h_e,\tau}(t=2)$ with different τ (lower part) for the LFFD method (2.6). Tables 5.2-5.6 show similar results for the SIFD1 method (2.7), SIFD2 method (2.8), CNFD method (2.9), EWI-FP method (3.18)-(3.19) and TSFP method (4.9) under different ε-scalability, respectively. For the LFFD and SIFD1 methods, due to the stability condition and accuracy requirement, we take

$$\delta_j(\varepsilon) = \begin{cases} \varepsilon^2 & \varepsilon_0/2^j \le \varepsilon \le 1, \\ \varepsilon_0^2/4^j & 0 < \varepsilon < \varepsilon_0/2^j, \end{cases} \qquad j = 0, 1, \ldots$$

in Tables 5.1 and 5.2. For comparison, Table 5.7 depicts temporal errors of different numerical methods when $\varepsilon = 1$ for different τ, and Table 5.8 shows the ε-scalability of different methods in the nonrelativistic limit regime.

From Tables 5.1-5.8, we can draw the following conclusions for the NLDE by using different numerical methods:

(i). For the discretization error in space, for any fixed $\varepsilon = \varepsilon_0 > 0$, the FDTD methods are second-order accurate, and resp., the EWI-FP and TSFP methods are spectrally accurate (cf. each row in the upper

Table 5.3: Spatial and temporal error analysis of the SIFD2 method for the NLDE (1.14).

Spatial Errors	$h_0 = 1/8$	$h_0/2$	$h_0/2^2$	$h_0/2^3$	$h_0/2^4$
$\varepsilon_0 = 1$	8.15E-2	2.02E-2	5.00E-3	1.25E-3	3.12E-4
order	-	2.01	2.01	2.00	2.00
$\varepsilon_0/2$	9.29E-2	2.30E-2	5.73E-3	1.43E-3	3.58E-4
order	-	2.01	2.01	2.00	2.00
$\varepsilon_0/2^2$	9.91E-2	2.46E-2	6.12E-3	1.53E-3	3.82E-4
order	-	2.01	2.01	2.00	2.00
$\varepsilon_0/2^3$	9.89E-2	2.47E-2	6.17E-3	1.54E-3	3.85E-4
order	-	2.00	2.00	2.00	2.00
$\varepsilon_0/2^4$	9.87E-2	2.48E-2	6.18E-3	1.54E-3	3.83E-4
order	-	1.99	2.00	2.00	2.01
Temporal Errors	$\tau_0 = 0.1$	$\tau_0/8$	$\tau_0/8^2$	$\tau_0/8^3$	$\tau_0/8^4$
$\varepsilon_0 = 1$	1.31E-1	2.10E-3	3.27E-5	5.11E-7	7.98E-9
order	-	1.99	2.00	2.00	2.00
$\varepsilon_0/2$	1.28	2.41E-2	3.78E-4	5.91E-6	9.23E-8
order	-	1.91	2.00	2.00	2.00
$\varepsilon_0/2^2$	2.34	8.99E-1	1.45E-2	2.30E-4	3.61E-6
order	-	0.46	1.98	1.99	2.00
$\varepsilon_0/2^3$	2.46	2.94	8.19E-1	1.30E-2	2.04E-4
order	-	-0.09	0.61	1.99	2.00
$\varepsilon_0/2^4$	2.79	3.15	4.28E-1	8.02E-1	1.26E-2
order	-	-0.06	0.96	-0.30	2.00

parts of Tables 5.1-5.6). For $0 < \varepsilon \leq 1$, the errors are independent of ε for the EWI-FP and TSFP methods (cf. each column in the upper parts of Tables 5.5-5.6), and resp., are almost independent of ε for the FDTD methods (cf. each column in the upper parts of Tables 5.1-5.4). In general, for any fixed $0 < \varepsilon \leq 1$ and $h > 0$, the EWI-FP and TSFP methods perform much better than the FDTD methods in spatial discretization.

(ii). For the discretization error in time, in the $O(1)$ speed-of-light regime, i.e. $\varepsilon = O(1)$, all the numerical methods including FDTD, EWI-FP and TSFP are second-order accurate (cf. the first row in the lower parts of Tables 5.1-5.6). In general, the TSFP method performs much better than the FDTD and EWI-FP methods in temporal discretization for a fixed time step (cf. Table 5.7). In the non-relativistic limit regime, i.e. $0 < \varepsilon \ll 1$, for the FDTD methods, the 'correct' ε-scalability is $\tau = O(\varepsilon^3)$ which verifies our theoretical results; for the EWI-FP and TSFP methods, the 'correct' ε-scalability is $\tau = O(\varepsilon^2)$ which again confirms our theoretical results. In fact, for $0 < \varepsilon \leq 1$, one can observe clearly second-order convergence in time for the FDTD methods only when $\tau \lesssim \varepsilon^3$ (cf. upper triangles in the lower parts of Tables 5.1-5.4), and resp., for the EWI-FP and TSFP methods when $\tau \lesssim \varepsilon^2$ (cf. upper triangles in the lower parts of Tables 5.5-5.6). In general, for any fixed $0 < \varepsilon \leq 1$ and $\tau > 0$, the TSFP method performs the best, and the EWI-FP method performs much better than the FDTD methods in temporal discretization (cf. Tables 5.7&5.8).

(iii). From Table 5.6, our numerical results suggest the following error bound for the TSFP method, i.e. there exist constants $h_0 > 0$ and $\tau_0 > 0$ sufficiently small and independent of ε, such that for any $0 < \varepsilon \leq 1$, when $0 < h \leq h_0$ and $0 < \tau \leq \tau_0$ satisfying $0 < \tau \lesssim \varepsilon^2 h^{1/4}$,

$$\|I_M(\Phi^n) - \Phi(t_n, \cdot)\|_{L^2} \lesssim h^{m_0} + \frac{\tau^2}{\varepsilon^2}, \qquad \|\Phi^n\|_{l^\infty} \lesssim 1 + M_0, \qquad 0 \leq n \leq \frac{T}{\tau}. \tag{5.18}$$

which is much better than (3) for the TSFP method in the nonrelativistic limit regime. Rigorous mathematical justification for (5.18) is on-going.

Similar to the FDTD methods for the Dirac equation [11], we can observe numerically the ε-dependence

Table 5.4: Spatial and temporal error analysis of the CNFD method for the NLDE (1.14).

Spatial Errors	$h_0 = 1/8$	$h_0/2$	$h_0/2^2$	$h_0/2^3$	$h_0/2^4$
$\varepsilon_0 = 1$	8.15E-2	2.02E-2	5.00E-3	1.25E-3	3.12E-4
order	-	2.01	2.01	2.00	2.00
$\varepsilon_0/2$	9.29E-2	2.30E-2	5.73E-2	1.43E-3	3.58E-4
order	-	2.01	2.01	2.00	2.00
$\varepsilon_0/2^2$	9.91E-2	2.46E-2	6.12E-3	1.53E-3	3.82E-4
order	-	2.01	2.01	2.00	2.00
$\varepsilon_0/2^3$	9.89E-2	2.47E-2	6.17E-3	1.54E-3	3.85E-4
order	-	2.00	2.00	2.00	2.00
$\varepsilon_0/2^4$	9.87E-2	2.48E-2	6.18E-3	1.54E-3	3.83E-4
order	-	1.99	2.00	2.00	2.01
Temporal Errors	τ_0=0.1	$\tau_0/8$	$\tau_0/8^2$	$\tau_0/8^3$	$\tau_0/8^4$
$\varepsilon_0 = 1$	7.13E-2	9.76E-4	1.52E-5	2.38E-7	3.65E-9
order	-	2.01	2.00	2.00	2.01
$\varepsilon_0/2$	4.58E-1	7.75E-3	1.21E-4	1.89E-6	2.95E-8
order	-	1.96	2.00	2.00	2.00
$\varepsilon_0/2^2$	1.74	2.34E-1	3.86E-3	6.01E-5	9.42E-7
order	-	0.96	1.97	2.00	2.00
$\varepsilon_0/2^3$	3.13	5.25E-1	2.07E-1	3.49E-3	5.46E-5
order	-	0.86	0.45	1.96	2.00
$\varepsilon_0/2^4$	2.34	1.84	8.16E-1	2.04E-1	3.42E-3
order	-	0.16	0.39	0.67	1.97

Table 5.5: Spatial and temporal error analysis of the EWI-FP method for the NLDE (1.14).

Spatial Errors	h_0=2	$h_0/2$	$h_0/2^2$	$h_0/2^3$	$h_0/2^4$
$\varepsilon_0 = 1$	1.68	4.92E-1	4.78E-2	1.40E-4	2.15E-9
$\varepsilon_0/2$	1.48	3.75E-1	1.57E-2	4.24E-5	6.60E-10
$\varepsilon_0/2^2$	1.21	2.90E-1	4.66E-3	4.91E-6	6.45E-10
$\varepsilon_0/2^3$	1.37	2.68E-1	2.40E-3	6.00E-7	6.34E-10
$\varepsilon_0/2^4$	1.41	2.75E-1	1.84E-3	3.06E-7	6.13E-10
$\varepsilon_0/2^5$	1.45	2.76E-1	1.74E-3	2.37E-7	5.98E-10
Temporal Errors	τ_0=0.1	$\tau_0/4$	$\tau_0/4^2$	$\tau_0/4^3$	$\tau_0/4^4$	$\tau_0/4^5$
$\varepsilon_0 = 1$	1.62E-1	8.75E-3	5.44E-4	3.40E-5	2.12E-6	1.33E-7
order	-	2.11	2.00	2.00	2.00	2.00
$\varepsilon_0/2$	2.02	2.58E-2	1.59E-3	9.94E-5	6.21E-6	3.88E-7
order	-	3.15	2.01	2.00	2.00	2.00
$\varepsilon_0/2^2$	2.11	2.11	1.12E-2	6.94E-4	4.33E-5	2.71E-6
order	-	0.00	3.78	2.01	2.00	2.00
$\varepsilon_0/2^3$	2.12	2.12	1.52E-1	8.88E-3	5.53E-4	3.45E-5
order	-	0.00	1.90	2.05	2.00	2.00
$\varepsilon_0/2^4$	2.06	2.06	2.06	1.40E-1	8.24E-3	5.13E-4
order	-	0.00	0.00	1.94	2.04	2.00
$\varepsilon_0/2^5$	2.09	2.03	2.03	2.03	1.36E-1	8.01E-3
order	-	0.02	0.00	0.00	1.95	2.04

in the spatial discretization error, i.e. $\frac{1}{\varepsilon}$ in front of h^2, which was proven in Theorems 2.1-2.4. Again, the

Table 5.6: Spatial and temporal error analysis of the TSFP method for the NLDE (1.14).

Spatial Errors	h_0=2	$h_0/2$	$h_0/2^2$	$h_0/2^3$	$h_0/2^4$
$\varepsilon_0 = 1$	1.68	4.92E-1	4.78E-2	1.40E-4	2.15E-9
$\varepsilon_0/2$	1.48	3.75E-1	1.57E-2	4.24E-5	6.60E-10
$\varepsilon_0/2^2$	1.21	2.90E-1	4.66E-3	4.91E-6	6.45E-10
$\varepsilon_0/2^3$	1.37	2.68E-1	2.40E-3	6.00E-7	6.34E-10
$\varepsilon_0/2^4$	1.41	2.75E-1	1.84E-3	3.06E-7	6.13E-10
$\varepsilon_0/2^5$	1.45	2.76E-1	1.74E-3	2.37E-7	5.98E-10

Temporal Errors	τ_0=0.4	$\tau_0/4$	$\tau_0/4^2$	$\tau_0/4^3$	$\tau_0/4^4$	$\tau_0/4^5$
$\varepsilon_0 = 1$	1.60E-1	9.56E-3	5.95E-4	3.72E-5	2.32E-6	1.46E-7
order	-	2.03	2.00	2.00	2.00	2.00
$\varepsilon_0/2$	8.94E-1	3.91E-2	2.40E-3	1.50E-4	9.36E-6	5.87E-7
order	-	2.26	2.01	2.00	2.00	2.00
$\varepsilon_0/2^2$	2.60	2.18E-1	1.06E-2	6.56E-4	4.09E-5	2.56E-6
order	-	1.79	2.18	2.01	2.00	2.00
$\varepsilon_0/2^3$	2.28	2.33	4.84E-2	2.58E-3	1.60E-4	9.98E-6
order	-	-0.02	2.79	2.11	2.01	2.00
$\varepsilon_0/2^4$	1.46	1.28	1.30	1.15E-2	6.19E-4	3.84E-5
order	-	0.10	-0.01	3.41	2.11	2.01
$\varepsilon_0/2^5$	1.53	3.27E-1	4.06E-1	4.13E-1	2.83E-3	1.53E-4
order	-	1.11	-0.16	-0.01	3.59	2.10

Table 5.7: Comparison of temporal errors of different methods for the NLDE (1.14) with $\varepsilon = 1$.

$\varepsilon = 1$	τ_0=0.1	$\tau_0/2$	$\tau_0/2^2$	$\tau_0/2^3$	$\tau_0/2^4$	$\tau_0/2^5$
LFFD	1.95E-1	4.39E-2	1.07E-2	2.67E-3	6.66E-4	1.66E-4
order	-	2.15	2.04	2.00	2.00	2.00
SIFD1	1.69E-1	4.19E-2	1.04E-2	2.61E-3	6.52E-4	1.63E-4
order	-	2.01	2.01	1.99	2.00	2.00
SIFD2	1.31E-1	3.34E-2	8.40E-3	2.10E-3	5.26E-4	1.31E-4
order	-	1.97	1.99	2.00	2.00	2.01
CNFD	7.13E-2	1.82E-2	4.55E-3	1.14E-3	2.84E-4	7.11E-5
order	-	1.97	2.00	2.00	2.01	2.00
EWI-FP	1.62E-1	3.56E-2	8.75E-3	2.18E-3	5.44E-4	1.36E-4
order	-	2.19	2.02	2.00	2.00	2.00
TSFP	9.56E-3	2.40E-3	6.56E-4	1.60E-4	3.84E-5	9.47E-6
order	-	1.99	1.87	2.04	2.06	2.02

details are omitted here for brevity.

Based on the above comparison, in view of both temporal and spatial accuracy and ε-scalability, we conclude that the TSFP and EWI-FP methods perform much better than the FDTD methods for the discretization of the NLDE (1.14) (or (1.4)), especially in the nonrelativistic limit regime. For the reader's convenience, we summarize the properties of different numerical methods for the NLDE in Table 5.9.

As observed in [14, 15], the time-splitting spectral (TSSP) method for the nonlinear Schrödinger equation (NLSE) performs much better for the physical observable, e.g. density and current, than for the wave function, in the semiclassical limit regime with respect to the scaled Planck constant $0 < \varepsilon \ll 1$. In order to see whether this is still valid for the TSFP method for the NLDE in the nonrelativistic limit regime, let

Table 5.8: Comparison of temporal errors of different numerical methods for the NLDE (1.14) under proper ε-scalability.

$\tau = O(\varepsilon^3)$, $h = O(\varepsilon)$	$\varepsilon_0 = 1$, $h_0 = 1/8$, $\tau_0 = 0.1$	$\varepsilon_0/2$, $h_0/2$, $\tau_0/8$	$\varepsilon_0/2^2$, $h_0/2^2$, $\tau_0/8^2$	$\varepsilon_0/2^3$, $h_0/2^3$, $\tau_0/8^3$	$\varepsilon_0/2^4$, $h_0/2^4$, $\tau_0/8^4$
LFFD	1.95E-1	1.42E-2	7.13E-3	6.45E-3	6.32E-3
Order in time	-	1.26	0.33	0.05	0.01
SIFD1	1.69E-1	2.08E-2	1.32E-2	1.26E-2	1.25E-2
Order in time	-	1.01	0.22	0.02	0.00
$\tau = O(\varepsilon^3)$	$\varepsilon_0 = 1$, $\tau_0 = 0.1$	$\varepsilon_0/2$, $\tau_0/8$	$\varepsilon_0/2^2$, $\tau_0/8^2$	$\varepsilon_0/2^3$, $\tau_0/8^3$	$\varepsilon_0/2^4$, $\tau_0/8^4$
SIFD2	1.31E-1	2.41E-2	1.45E-2	2.30E-2	1.26E-2
Order in time	-	0.81	0.24	-0.22	0.29
CNFD	7.13E-2	7.75E-3	3.86E-3	3.49E-3	3.42E-3
Order in time	-	1.07	0.34	0.05	0.01
$\tau = O(\varepsilon^2)$	$\varepsilon_0 = 1$, $\tau_0 = 0.1$	$\varepsilon_0/2$, $\tau_0/4$	$\varepsilon_0/2^2$, $\tau_0/4^2$	$\varepsilon_0/2^3$, $\tau_0/4^3$	$\varepsilon_0/2^4$, $\tau_0/4^4$
EWI-FP	1.62E-1	2.58E-2	1.12E-2	8.88E-3	8.24E-3
Order in time	-	1.33	0.60	0.17	0.05
TSFP	9.56E-3	2.40E-3	6.56E-4	1.60E-4	3.84E-5
Order in time	-	1.00	0.94	1.02	1.03

Table 5.9: Comparison of properties of different numerical methods for solving the NLDE (1.14) (or (1.4)) with M being the number of grid points in space.

Method	LFFD	SIFD1	SIFD2	CNFD	EWI-FP	TSFP
Time symmetric	Yes	Yes	Yes	Yes	No	Yes
Mass conservation	No	No	No	Yes	No	Yes
Energy conservation	No	No	No	Yes	No	No
Dispersion relation	No	No	No	No	No	Yes
Time transverse invariant	No	No	No	No	No	Yes
Unconditionally stable	No	No	Yes	Yes	No	Yes
Explicit scheme	Yes	No	No	No	Yes	Yes
Temporal accuracy	2nd	2nd	2nd	2nd	2nd	2nd
Spatial accuracy	2nd	2nd	2nd	2nd	Spectral	Spectral
Memory cost	$O(M)$	$O(M)$	$O(M)$	$O(M)$	$O(M)$	$O(M)$
Computational cost	$O(M)$	$O(M)$	$> O(M)$	$\gg O(M)$	$O(M \ln M)$	$O(M \ln M)$
Resolution when $0 < \varepsilon \ll 1$	$h = O(\sqrt{\varepsilon})$, $\tau = O(\varepsilon^3)$	$h = O(\sqrt{\varepsilon})$, $\tau = O(\varepsilon^3)$	$h = O(\sqrt{\varepsilon})$, $\tau = O(\varepsilon^3)$	$h = O(\sqrt{\varepsilon})$, $\tau = O(\varepsilon^3)$	$h = O(1)$, $\tau = O(\varepsilon^2)$	$h = O(1)$, $\tau = O(\varepsilon^2)$

$\rho^n = |\Phi^n_{h,\tau}|^2$, $\mathbf{J}^n = \frac{1}{\varepsilon}(\Phi^n_{h,\tau})^* \sigma_1 \Phi^n_{h,\tau}$ with $\Phi^n_{h,\tau}$ the numerical solution obtained by the TSFP method with mesh size h and time step τ, and define the errors

$$e_\rho^{h,\tau}(t_n) := \|\rho^n - \rho(t_n,\cdot)\|_{l^1} = h\sum_{j=0}^{N-1} |\rho_j^n - \rho(t_n,x_j)|, \quad e_{\mathbf{J}}^{h,\tau}(t_n) := \|\mathbf{J}^n - \mathbf{J}(t_n,\cdot)\|_{l^1} = h\sum_{j=0}^{N-1} |\mathbf{J}_j^n - \mathbf{J}(t_n,x_j)|.$$

Table 5.10 lists temporal errors $e_\rho^{h,\tau}(t=2)$ and $e_{\mathbf{J}}^{h,\tau}(t=2)$ with different τ for the TSFP method (4.9). From this Table, we can see that the approximations of the density and current are at the same order as for the wave function by using the TSFP method. The reason that we can speculate is that $\rho = O(1)$ and $\mathbf{J} = O(\varepsilon^{-1})$ (see details in (1.7) or (1.17)) in the NLDE, while in the NLSE both density and current are

Table 5.10: Temporal errors for density and current of the TSFP for the Dirac equation (1.14) in 1D.

$e_\rho^{h,\tau}(t=2)$	τ_0=0.4	$\tau_0/4$	$\tau_0/4^2$	$\tau_0/4^3$	$\tau_0/4^4$	$\tau_0/4^5$	$\tau_0/4^6$
$\varepsilon_0=1$	2.43E-1	1.51E-2	9.40E-4	5.88E-5	3.67E-6	2.29E-7	1.42E-8
order	-	2.00	2.00	2.00	2.00	2.00	2.01
$\varepsilon_0/2$	1.08	3.32E-2	2.04E-3	1.28E-4	7.98E-6	4.98E-7	3.09E-8
order	-	2.51	2.01	2.00	2.00	2.00	2.01
$\varepsilon_0/2^2$	1.53	1.67E-1	7.68E-2	4.72E-4	2.95E-5	1.84E-6	1.16E-7
order	-	1.60	0.56	3.67	2.00	2.00	1.99
$\varepsilon_0/2^3$	1.30	1.27	2.14E-2	9.68E-4	5.95E-5	3.72E-6	2.32E-7
order	-	0.02	2.95	2.23	2.01	2.00	1.99
$\varepsilon_0/2^4$	1.25	9.44E-1	9.40E-1	5.81E-3	2.74E-4	1.69E-5	1.06E-6
order	-	0.20	0.00	3.67	2.20	2.01	2.00
$\varepsilon_0/2^5$	1.13	3.41E-1	3.27E-1	3.27E-1	1.38E-3	6.58E-5	4.06E-6
order	-	0.20	0.86	0.03	3.94	2.20	2.01
$e_{\mathbf{J}}^{h,\tau}(t=2)$	τ_0=0.4	$\tau_0/4$	$\tau_0/4^2$	$\tau_0/4^3$	$\tau_0/4^4$	$\tau_0/4^5$	$\tau_0/4^6$
$\varepsilon_0=1$	1.23E-1	7.20E-3	4.47E-4	2.79E-5	1.74E-6	1.09E-7	6.73E-9
order	-	2.05	2.00	2.00	2.00	2.00	2.01
$\varepsilon_0/2$	9.64E-1	4.38E-2	2.67E-3	1.67E-4	1.04E-5	6.50E-7	4.07E-8
order	-	2.23	2.02	2.00	2.00	2.00	2.00
$\varepsilon_0/2^2$	1.91	1.81E-1	8.19E-3	5.03E-4	3.14E-5	1.96E-6	1.23E-7
order	-	1.70	2.23	2.01	2.00	2.00	2.00
$\varepsilon_0/2^3$	1.53	1.59	3.40E-2	1.65E-3	1.02E-4	6.37E-6	3.98E-7
order	-	-0.03	2.77	2.18	2.01	2.00	2.00
$\varepsilon_0/2^4$	1.00	1.43	1.44	9.42E-3	5.04E-4	3.13E-5	1.95E-6
order	-	-0.26	-0.01	3.63	2.11	2.00	2.00
$\varepsilon_0/2^5$	1.24	3.10E-1	3.71E-1	3.76E-1	1.59E-3	8.48E-5	5.26E-6
order	-	1.00	-0.13	-0.01	3.94	2.11	2.01

all at $O(1)$, when $0 < \varepsilon \ll 1$.

6. Conclusion

Three types of numerical methods based on different time integrations were analyzed rigorously and compared numerically for solving the nonlinear Dirac equation (NLDE) in the nonrelativistic limit regime, i.e. $0 < \varepsilon \ll 1$. The first class consists of the second order standard FDTD methods, including LFFD, SIFD1, SIFD2 and CNFD. The error estimates of the FDTD methods were rigorously analyzed, which suggest that the ε-scalability of the FDTD methods is $\tau = O(\varepsilon^3)$ and $h = O(\sqrt{\varepsilon})$. The second class applies the Fourier spectral discretization in space and Gautschi-type integration in time, resulting in the EWI-FP method. Rigorous error bounds for the EWI-FP method were derived, which show that the ε-scalability of the EWI-FP method is $\tau = O(\varepsilon^2)$ and $h = O(1)$. The last class combines the Fourier spectral discretization in space and time-splitting technique in time, which leads to the TSFP method. Based on the rigorous error analysis, the ε-scalability of the TSFP method is $\tau = O(\varepsilon^2)$ and $h = O(1)$, which is similar to the EWI-FP method. From the error analysis and numerical results, the TSFP and EWI-FP methods perform much better than the FDTD methods, especially in the nonrelativistic limit regime. Extensive numerical results indicate that the TSFP method is superior than the EWI-FP in terms of accuracy and efficiency, and thus the TSFP method is favorable for solving the NLDE directly, especially in the nonrelativistic limit regime.

Appendix A. Proof of Theorem 2.1 for the CNFD method

Proof. Comparison to the proof of the CNFD method for the Dirac equation in [11], the main difficulty is to show the numerical solution Φ^n is uniformly bounded, i.e. $\|\Phi^n\|_{l^\infty} \lesssim 1$. In order to do so, we adapt the cut-off technique to truncate the nonlinearity $\mathbf{F}(\Phi)$ to a global Lipschitz function with compact support [8, 9, 10]. Choose a smooth function $\alpha(\rho)(\rho \geq 0) \in C^\infty([0,\infty))$ defined as

$$\alpha(\rho) = \begin{cases} 1, & 0 \leq \rho \leq 1, \\ \in [0,1], & 1 \leq \rho \leq 2, \\ 0, & \rho \geq 2. \end{cases}$$

Denote $M_1 = 2(1+M_0)^2 > 0$ and define

$$\mathbf{F}_{M_1}(\Phi) = \alpha\left(\frac{|\Phi|^2}{M_1}\right)\mathbf{F}(\Phi), \qquad \Phi \in \mathbb{C}^2, \tag{A.1}$$

then $\mathbf{F}_{M_1}(\Phi)$ has compact support and is smooth and global Lipschitz, i.e.,

$$\|\mathbf{F}_{M_1}(\Phi_1) - \mathbf{F}_{M_1}(\Phi_2)\| \leq C_{M_1}\Big|\,|\Phi_1| - |\Phi_2|\,\Big| \lesssim \Big|\,|\Phi_1| - |\Phi_2|\,\Big|, \qquad \Phi_1, \Phi_2 \in \mathbb{C}^2, \tag{A.2}$$

where C_{M_1} is a constant independent of ε, h and τ. Choose $\widetilde{\Phi}^n \in X_M$ $(n \geq 0)$ such that $\widetilde{\Phi}^0 = \Phi^0$ and $\widetilde{\Phi}^n$ $(n \geq 1)$, with $\widetilde{\Phi}^n = (\widetilde{\Phi}_0^n, \widetilde{\Phi}_1^n, \ldots, \widetilde{\Phi}_M^n)^T$ and $\widetilde{\Phi}_j^n = (\widetilde{\phi}_{1,j}^n, \widetilde{\phi}_{2,j}^n)^T$ for $j = 0, 1, ...M$, be the numerical solution of the following finite difference equation

$$i\delta_t^+\tilde{\Phi}_j^n = \left[-\frac{i}{\varepsilon}\sigma_1\delta_x + \frac{1}{\varepsilon^2}\sigma_3 + V_j^{n+1/2}I_2 - A_{1,j}^{n+1/2}\sigma_1 + \mathbf{F}_{M_1,j}^{n+1/2}\right]\tilde{\Phi}_j^{n+1/2}, \quad 0 \leq j \leq M-1,\ n \geq 0, \tag{A.3}$$

where $\tilde{\Phi}_j^{n+1/2} = \frac{1}{2}\left[\tilde{\Phi}_j^n + \tilde{\Phi}_j^{n+1}\right]$ and $\mathbf{F}_{M_1,j}^{n+1/2} = \frac{1}{2}\left[\mathbf{F}_{M_1}(\tilde{\Phi}_j^n) + \mathbf{F}_{M_1}(\tilde{\Phi}_j^{n+1})\right]$ for $j = 0, 1, \ldots, M$. In fact, we can view $\widetilde{\Phi}^n$ as another approximation to $\Phi(t_n, x)$. Define the corresponding errors:

$$\widetilde{\mathbf{e}}_j^n = \Phi(t_n, x_j) - \widetilde{\Phi}_j^n, \qquad j = 0, 1, ..., M, \qquad n \geq 0$$

Then the local truncation error $\widetilde{\xi}^n \in X_M$ of the scheme (A.3) is defined as

$$\widetilde{\xi}_j^n := i\delta_t^+\Phi(t_n, x_j) - \left[-\frac{i}{\varepsilon}\sigma_1\delta_x + \frac{1}{\varepsilon^2}\sigma_3 + V_j^{n+1/2}I_2 - A_{1,j}^{n+1/2}\sigma_1 + \mathbf{W}_j^n(\Phi)\right]\frac{\Phi(t_{n+1}, x_j) + \Phi(t_n, x_j)}{2}, \tag{A.4}$$

where

$$\mathbf{W}_j^n(\Phi) = \frac{1}{2}\left[\mathbf{F}_{M_1}(\Phi(t_n, x_j)) + \mathbf{F}_{M_1}(\Phi(t_{n+1}, x_j))\right], \qquad j = 0, 1, \ldots, M, \quad n \geq 0. \tag{A.5}$$

Taking the Taylor expansion in the local truncation error (A.4), noticing (2.1) and (A.1), under the assumptions of (A) and (B), with the help of triangle inequality and Cauchy-Schwartz inequality, we have

$$\begin{aligned} |\widetilde{\xi}_j^n| \leq & \frac{\tau^2}{24}\|\partial_{ttt}\Phi\|_{L^\infty(\overline{\Omega}_T)} + \frac{h^2}{6\varepsilon}\|\partial_{xxx}\Phi\|_{L^\infty(\overline{\Omega}_T)} + \frac{\tau^2}{8\varepsilon}\|\partial_{xtt}\Phi\|_{L^\infty(\overline{\Omega}_T)} \\ & + \frac{\tau^2}{8}\left(\frac{1}{\varepsilon^2} + 2 + 2(|\lambda_1| + |\lambda_2|)M_0^2 + V_{\max} + A_{1,\max}\right)\|\partial_{tt}\Phi\|_{L^\infty(\overline{\Omega}_T)} \\ \lesssim & \frac{\tau^2}{\varepsilon^6} + \frac{h^2}{\varepsilon} + \frac{\tau^2}{\varepsilon^5} + \frac{\tau^2}{\varepsilon^6} \lesssim \frac{\tau^2}{\varepsilon^6} + \frac{h^2}{\varepsilon}, \qquad j = 0, 1, \ldots, M-1, \quad n \geq 0. \end{aligned} \tag{A.6}$$

Subtracting (A.4) from (A.3), we can obtain

$$i\delta_t^+\widetilde{\mathbf{e}}_j^n = \left[-\frac{i}{\varepsilon}\sigma_1\delta_x + \frac{1}{\varepsilon^2}\sigma_3 + V_j^{n+1/2}I_2 - A_{1,j}^{n+1/2}\sigma_1\right]\tilde{\mathbf{e}}_j^{n+1/2} + \widetilde{\xi}_j^n + \tilde{\eta}_j^n, \quad 0 \leq j \leq M-1, \quad n \geq 0, \tag{A.7}$$

where $\tilde{\mathbf{e}}_j^{n+1/2} = \frac{1}{2}\left[\tilde{\mathbf{e}}_j^n + \tilde{\mathbf{e}}_j^{n+1}\right]$ and

$$\widetilde{\eta}_j^n = \frac{1}{2}\mathbf{W}_j^n(\Phi)\left[\Phi(t_{n+1}, x_j) + \Phi(t_n, x_j)\right] - \mathbf{F}_{M_1,j}^{n+1/2}\tilde{\Phi}_j^{n+1/2}, \quad 0 \le j \le M-1, \quad n \ge 0. \tag{A.8}$$

Combining (A.8), (A.5) and (A.2), we get

$$\left|\tilde{\eta}_j^n\right| \lesssim |\widetilde{\mathbf{e}}_j^{n+1}| + |\widetilde{\mathbf{e}}_j^n|, \qquad 0 \le j \le M-1, \quad n \ge 0. \tag{A.9}$$

Multiplying both sides of (A.7) by $h(\widetilde{\mathbf{e}}_j^{n+\frac{1}{2}})^*$, summing them up for $j = 0, 1, .., M-1$, taking imaginary parts and applying the Cauchy inequality, noticing (A.6), we can have

$$\begin{aligned} \|\widetilde{\mathbf{e}}^{n+1}\|_{l^2}^2 - \|\widetilde{\mathbf{e}}^n\|_{l^2}^2 &\lesssim \tau\left(\|\widetilde{\xi}^n\|_{l^2}^2 + \|\widetilde{\xi}^n\|_{l^2}^2 + \|\widetilde{\mathbf{e}}^{n+1}\|_{l^2}^2 + \|\widetilde{\mathbf{e}}^n\|_{l^2}^2\right) \\ &\lesssim \tau\left[\left(\frac{h^2}{\varepsilon} + \frac{\tau^2}{\varepsilon^6}\right)^2 + \|\widetilde{\mathbf{e}}^{n+1}\|_{l^2}^2 + \|\widetilde{\mathbf{e}}^n\|_{l^2}^2\right], \qquad n \ge 0. \end{aligned} \tag{A.10}$$

Summing the above inequality, we obtain

$$\|\widetilde{\mathbf{e}}^n\|_{l^2}^2 - \|\widetilde{\mathbf{e}}^0\|_{l^2}^2 \lesssim \tau\sum_{l=0}^{n}\|\widetilde{\mathbf{e}}^l\|_{l^2}^2 + \left(\frac{h^2}{\varepsilon} + \frac{\tau^2}{\varepsilon^6}\right)^2, \qquad 0 \le n \le \frac{T}{\tau}. \tag{A.11}$$

Using the discrete Gronwall's inequality and noting $\widetilde{\mathbf{e}}^0 = \mathbf{0}$, there exist $0 < \tau_1 \le \frac{1}{2}$ and $h_1 > 0$ sufficiently small and independent of ε, when $0 < \tau \le \tau_1$ and $0 < h \le h_1$, we get

$$\|\widetilde{\mathbf{e}}^n\|_{l^2} \lesssim \frac{h^2}{\varepsilon} + \frac{\tau^2}{\varepsilon^6}, \qquad 0 \le n \le \frac{T}{\tau}. \tag{A.12}$$

Applying the inverse inequality in 1D, we have

$$\|\widetilde{\mathbf{e}}^n\|_{l^\infty} \lesssim \frac{1}{\sqrt{h}}\|\widetilde{\mathbf{e}}^n\|_{l^2} \lesssim \frac{h^{\frac{3}{2}}}{\varepsilon} + \frac{\tau^2}{\varepsilon^6\sqrt{h}}, \qquad 0 \le n \le \frac{T}{\tau}. \tag{A.13}$$

Under the conditions $0 < \tau \lesssim \varepsilon^3 h^{\frac{1}{4}}$ and $0 < h \lesssim \varepsilon^{2/3}$, there exist $h_2 > 0$ and $\tau_2 > 0$ sufficiently small and independent of ε, when $0 < h \le h_2$ and $0 < \tau \le \tau_2$, we get

$$\|\widetilde{\Phi}^n\|_{l^\infty} \le \|\Phi\|_{L^\infty(\Omega_T)} + \|\widetilde{\mathbf{e}}^n\|_{l^\infty} \le 1 + M_0, \qquad 0 \le n \le \frac{T}{\tau}. \tag{A.14}$$

Therefore, under the conditions in Theorem 2.1, the discretization (A.3) collapses exactly to the CNFD discretization (2.9) for the NLDE if we take $\tau_0 = \min\{1/2, \tau_1, \tau_2\}$ and $h_0 = \min\{h_1, h_2\}$, i.e.

$$\widetilde{\Phi}^n = \Phi^n, \qquad 0 \le n \le \frac{T}{\tau}. \tag{A.15}$$

Thus the proof is completed. □

Appendix B. Proof of Theorem 2.2 for the LFFD method

Proof. Again, comparison to the proof of the LFFD method for the Dirac equation in [11], the main difficulty is to show the numerical solution Φ^n is uniformly bounded, i.e. $\|\Phi^n\|_{l^\infty} \lesssim 1$. In order to do

so, we adapt the method of mathematical induction [8, 9, 10]. Define the local truncation error $\hat{\xi}^n = (\hat{\xi}_0^n, \hat{\xi}_1^n, \ldots, \hat{\xi}_M^n)^T \in X_M$ $(n \geq 0)$ of the LFFD method (2.6) with (2.11) as

$$\hat{\xi}_j^0 := i\delta_t^+ \Phi(0, x_j) + \frac{1}{\tau} \sin\left(\frac{\tau}{\varepsilon}\right) \sigma_1 \delta_x \Phi_0(x_j) + i\left(\frac{1}{\tau} \sin\left(\frac{\tau}{\varepsilon^2}\right) \sigma_3 + V_j^0 I_2 - A_{1,j}^0 \sigma_1 + \mathbf{F}(\Phi(0, x_j))\right) \Phi(0, x_j), \tag{B.1}$$

$$\hat{\xi}_j^n := i\delta_t \Phi(t_n, x_j) - \left[-\frac{i}{\varepsilon}\sigma_1 \delta_x + \frac{1}{\varepsilon^2}\sigma_3 + V_j^n I_2 - A_{1,j}^n \sigma_1 + \mathbf{F}(\Phi(t_n, x_j))\right] \Phi(t_n, x_j), \quad 0 \leq j < M, n \geq 1. \tag{B.2}$$

Similar to the proof of Theorem 2.1, applying the Taylor expansion, we obtain

$$|\hat{\xi}_j^0| \lesssim \frac{\tau}{\varepsilon^4} + \frac{h^2}{\varepsilon}, \qquad |\hat{\xi}_j^n| \lesssim \frac{\tau^2}{\varepsilon^6} + \frac{h^2}{\varepsilon}, \qquad j = 0, 1, ..., M-1, \qquad n \geq 1. \tag{B.3}$$

Subtracting (2.11) and (2.6) from (B.1) and (B.2), respectively, we get the error equations

$$i\delta_t \mathbf{e}_j^n = \left[-\frac{i}{\varepsilon}\sigma_1 \delta_x + \frac{1}{\varepsilon^2}\sigma_3 + V_j^n I_2 - A_{1,j}^n \sigma_1\right] \mathbf{e}_j^n + \eta_j^n + \hat{\xi}_j^n, \qquad 0 \leq j \leq M-1, \quad n \geq 1, \tag{B.4}$$

$$\mathbf{e}_j^1 = \tau \hat{\xi}_j^0 + \mathbf{e}_j^0, \qquad \mathbf{e}_j^0 = \Phi(0, x_j) - \Phi_j^0 = 0, \qquad j = 0, 1, \ldots, M-1, \tag{B.5}$$

where $\eta^n \in X_M$ is given as

$$\eta_j^n = \mathbf{F}(\Phi(t_n, x_j))\Phi(t_n, x_j) - \mathbf{F}(\Phi_j^n)\Phi_j^n, \qquad j = 0, 1, \ldots, M, \qquad n \geq 1. \tag{B.6}$$

From (B.5), we know that (2.25) is valid for $n = 0$. In addition, noticing (B.3) and assume $0 < \tau \leq 1$, we have

$$\|\mathbf{e}^1\|_{l^2} \lesssim \|\mathbf{e}^1\|_{l^\infty} \leq \tau \|\hat{\xi}^0\|_{l^\infty} \lesssim \frac{\tau^2}{\varepsilon^4} + \frac{\tau h^2}{\varepsilon} \lesssim \frac{\tau^2}{\varepsilon^6} + \frac{h^2}{\varepsilon}. \tag{B.7}$$

By using the inverse inequality, we get

$$\|\mathbf{e}^1\|_{l^\infty} \lesssim \frac{1}{h^{1/2}} \|\mathbf{e}^1\|_{l^2} \lesssim \frac{\tau^2}{\varepsilon^6 h^{1/2}} + \frac{h^{3/2}}{\varepsilon}. \tag{B.8}$$

Thus, under the conditions in Theorem 2.2, there exist $h_1 > 0$ and $\tau_1 > 0$ sufficiently small and independent of ε such that, for $0 < \varepsilon \leq 1$, when $0 < h \leq h_1$ and $0 < \tau \leq \tau_1$, we have

$$\|\Phi^1\|_{l^\infty} \leq \|\Phi(t_1, x)\|_{L^\infty} + \|\mathbf{e}^1\|_{l^\infty} \leq 1 + M_0, \tag{B.9}$$

which immediately implies that (2.25) is valid for $n = 1$.

Now we assume that (2.25) is valid for $0 \leq n \leq m \leq \frac{T}{\tau} - 1$. From (B.6), we have

$$\begin{aligned} |\eta_j^l| &= \left|F(\Phi(t_l, x_j))\Phi(t_l, x_j) - F(\Phi_j^l)\Phi_j^l\right| \\ &\leq \left\|F(\Phi(t_l, x_j)) - F(\Phi_j^l)\right\| \, |\Phi(t_l, x_j)| + \left\|F(\Phi_j^l)\right\| \, \left|\Phi(t_l, x_j) - \Phi_j^l\right| \\ &\lesssim |\mathbf{e}_j^l|, \qquad j = 0, 1, \ldots, M-1, \qquad l = 0, 1, \ldots, m. \end{aligned} \tag{B.10}$$

Denote $\mathcal{E}^l$ $(l \geq 0)$ as

$$\mathcal{E}^l = \|\mathbf{e}^{l+1}\|_{l^2}^2 + \|\mathbf{e}^l\|_{l^2}^2 + 2\,\mathrm{Re}\left(\tau h \sum_{j=0}^{M-1} (\mathbf{e}_j^{l+1})^* \sigma_1 \delta_x \mathbf{e}_j^l\right) - 2\,\mathrm{Im}\left(\frac{\tau h}{\varepsilon^2} \sum_{j=0}^{M-1} (\mathbf{e}_j^{l+1})^* \sigma_3 \mathbf{e}_j^l\right). \tag{B.11}$$

Under the stability condition (2.15) and the conditions in Theorem 2.2, for $0 < \varepsilon \leq 1$, when $\tau > 0$ and $h > 0$ satisfying $0 < \frac{\tau}{h} \leq \frac{1}{4}$ and $0 < \frac{\tau}{\varepsilon^2} \leq \frac{1}{4}$, using the Cauchy inequality, we obtain

$$\frac{1}{2}\left(\|\mathbf{e}^{l+1}\|_{l^2}^2 + \|\mathbf{e}^l\|_{l^2}^2\right) \leq \mathcal{E}^l \leq \frac{3}{2}\left(\|\mathbf{e}^{l+1}\|_{l^2}^2 + \|\mathbf{e}^l\|_{l^2}^2\right). \tag{B.12}$$

From (2.25) with $n = 0$ and $n = 1$, we have

$$\mathcal{E}^0 \lesssim \left(\frac{h^2}{\varepsilon} + \frac{\tau^2}{\varepsilon^6}\right)^2. \tag{B.13}$$

Multiplying both sides of (B.4) from the left by $2h\tau\left(\mathbf{e}_j^{n+1} + \mathbf{e}_j^{n-1}\right)^*$, taking the imaginary part, then summing for $j = 0, 1, \ldots, M-1$, using the Cauchy inequality, (B.3) and (B.12), we get

$$\begin{aligned}\mathcal{E}^l - \mathcal{E}^{l-1} \lesssim & h\tau \sum_{j=0}^{M-1} \left[(A_{1,\max} + V_{\max})|\mathbf{e}_j^l| + |\eta_j^n| + |\xi_j^l|\right]\left(|\mathbf{e}_j^{l+1}| + |\mathbf{e}_j^{l-1}|\right) \\ \lesssim & \tau(\mathcal{E}^l + \mathcal{E}^{l-1}) + \tau\left(\frac{h^2}{\varepsilon} + \frac{\tau^2}{\varepsilon^6}\right)^2, \qquad l \geq 1.\end{aligned}$$

Summing the above inequality for $l = 1, 2, \ldots, m$, we get

$$\mathcal{E}^m - \mathcal{E}^0 \lesssim \tau \sum_{l=0}^{m} \mathcal{E}^l + m\tau\left(\frac{h^2}{\varepsilon} + \frac{\tau^2}{\varepsilon^6}\right)^2.$$

There exist $0 < \tau_2 \leq \frac{1}{2}$ and $h_2 > 0$ sufficiently small and independent of ε, when $0 < \tau \leq \tau_2$ and $0 < h \leq h_2$, using the discrete Gronwall's inequality and noticing (B.13), we obtain

$$\|\mathbf{e}^{m+1}\|_{l^2}^2 \leq 2\mathcal{E}^m \lesssim \left(\frac{h^2}{\varepsilon} + \frac{\tau^2}{\varepsilon^6}\right)^2, \qquad 1 \leq m \leq \frac{T}{\tau} - 1. \tag{B.14}$$

In addition, by using the inverse inequality, we get

$$\|\mathbf{e}^{m+1}\|_{l^\infty} \lesssim \frac{1}{h^{1/2}}\|\mathbf{e}^{m+1}\|_{l^2} \lesssim \frac{\tau^2}{\varepsilon^6 h^{1/2}} + \frac{h^{3/2}}{\varepsilon}. \tag{B.15}$$

Thus, under the conditions in Theorem 2.2, there exist $h_3 > 0$ and $\tau_3 > 0$ sufficiently small and independent of ε such that, for $0 < \varepsilon \leq 1$, when $0 < h \leq h_3$ and $0 < \tau \leq \tau_3$, we have

$$\|\Phi^{m+1}\|_{l^\infty} \leq \|\Phi(t_{m+1}, x)\|_{L^\infty} + \|\mathbf{e}^{m+1}\|_{l^\infty} \leq 1 + M_0, \tag{B.16}$$

which immediately implies that (2.25) is valid for $n = m + 1$. Thus we complete the proof of Theorem 2.2 by taking $\tau_0 = \min\{1/4, \tau_1, \tau_2, \tau_3\}$ and $h_0 = \min\{1, h_1, h_2, h_3\}$. □

Appendix C. Proof of Theorem 3.1 for the EWI-FP method

Proof. Here the main difficulty is to show that the numerical solution $\Phi_M^n(x)$ is uniformly bounded, i.e. $\|\Phi_M^n(x)\|_{L^\infty} \lesssim 1$, which will be established by the method of mathematical induction [8, 9, 10]. Define the error function $\mathbf{e}^n(x) \in Y_M$ for $n \geq 0$ as

$$\mathbf{e}^n(x) = P_M\Phi(t_n, x) - \Phi_M^n(x) = \sum_{l=-M/2}^{M/2-1} \widehat{\mathbf{e}}_l^n e^{i\mu_l(x-a)}, \qquad a \leq x \leq b, \quad n \geq 0. \tag{C.1}$$

Using the triangular inequality and standard interpolation result, we get

$$\begin{aligned}\|\Phi(t_n, x) - \Phi_M^n(x)\|_{L^2} \leq & \|\Phi(t_n, x) - P_M\Phi(t_n, x)\|_{L^2} + \|\mathbf{e}^n(x)\|_{L^2} \\ \leq & h^{m_0} + \|\mathbf{e}^n(x)\|_{L^2}, \quad 0 \leq n \leq \frac{T}{\tau}.\end{aligned} \tag{C.2}$$

Thus we only need estimate $\|\mathbf{e}^n(x)\|_{L^2}$. It is easy to see that (3.21) is valid when $n=0$.

Define the local truncation error $\xi^n(x)=\sum_{l=-M/2}^{M/2-1}\widehat{\xi}_l^n e^{i\mu_l(x-a)}\in Y_M$ of the EWI-FP (3.15) for $n\geq 0$ as

$$\widehat{\xi}_l^n=\begin{cases}\widehat{(\Phi(\tau))}_l-e^{-i\tau\Gamma_l/\varepsilon^2}\widehat{(\Phi(0))}_l+i\varepsilon^2\Gamma_l^{-1}\left[I_2-e^{-\frac{i\tau}{\varepsilon^2}\Gamma_l}\right]\widehat{\mathbf{G}(\Phi)}_l(0), & n=0,\\ \widehat{(\Phi(t_{n+1}))}_l-e^{-i\tau\Gamma_l/\varepsilon^2}\widehat{(\Phi(t_n))}_l+iQ_l^{(1)}(\tau)\widehat{\mathbf{G}(\Phi)}_l(t_n)+iQ_l^{(2)}(\tau)\delta_t^-\widehat{\mathbf{G}(\Phi)}_l(t_n), & n\geq 1,\end{cases}\tag{C.3}$$

where we denote $\Phi(t)$ and $\mathbf{G}(\Phi)$ in short for $\Phi(t,x)$ and $\mathbf{G}(\Phi(t,x))$ in (3.17), respectively, for the simplicity of notations. In order to estimate the local truncation error $\xi^n(x)$, multiplying both sides of the NLDE (2.1) by $e^{i\mu_l(x-a)}$ and integrating over the interval (a,b), we easily recover the equations for $\widehat{\Phi(t)}_l$, which are exactly the same as (3.6) with Φ_M being replaced by $\Phi(t,x)$. Replacing Φ_M with $\Phi(t,x)$, we use the same notations $\widehat{\mathbf{G}(\Phi)}_l^n(s)$ as in (3.8) and the time derivatives of $\widehat{\mathbf{G}(\Phi)}_l^n(s)$ enjoy the same properties of time derivatives of $\Phi(t,x)$. Thus, the same representation (3.10) holds for $\widehat{\Phi(t_n)}_l$ for $n\geq 1$. From the derivation of the EWI-FS method, it is clear that the error $\xi^n(x)$ comes from the approximations for the integrals in (3.11) and (3.12). Thus we have

$$\widehat{\xi}_l^0=-i\int_0^\tau e^{\frac{i(s-\tau)}{\varepsilon^2}\Gamma_l}\left[\widehat{\mathbf{G}(\Phi)}_l^0(s)-\widehat{\mathbf{G}(\Phi)}_l^0(0)\right]ds=-i\int_0^\tau\int_0^s e^{\frac{i(s-\tau)}{\varepsilon^2}\Gamma_l}\partial_{s_1}\widehat{\mathbf{G}(\Phi)}_l^0(s_1)\,ds_1ds,\tag{C.4}$$

and for $n\geq 1$

$$\widehat{\xi}_l^n=-i\int_0^\tau e^{\frac{i(s-\tau)}{\varepsilon^2}\Gamma_l}\left(\int_0^s\int_0^{s_1}\partial_{s_2s_2}\widehat{\mathbf{G}(\Phi)}_l^n(s_2)\,ds_2ds_1+s\int_0^1\int_{\theta\tau}^\tau\partial_{\theta_1\theta_1}\widehat{\mathbf{G}(\Phi)}_l^{n-1}(\theta_1)\,d\theta_1d\theta\right)ds.\tag{C.5}$$

Subtracting (3.15) from (C.3), we obtain

$$\widehat{\mathbf{e}}_l^{n+1}=e^{-i\tau\Gamma_l/\varepsilon^2}\widehat{\mathbf{e}}_l^n+\widehat{R}_l^n+\widehat{\xi}_l^n,\qquad 1\leq n\leq\frac{T}{\tau}-1,\tag{C.6}$$

$$\widehat{\mathbf{e}}_l^0=\mathbf{0},\qquad \widehat{\mathbf{e}}_l^1=\widehat{\xi}_l^0,\qquad l=-\frac{M}{2},...,\frac{M}{2}-1.\tag{C.7}$$

where $R^n(x)=\sum_{l=-M/2}^{M/2-1}\widehat{R}_l^n e^{i\mu_l(x-a)}\in Y_M$ for $n\geq 1$ is given by

$$\widehat{R}_l^n=-iQ_l^{(1)}(\tau)\left[\widehat{\mathbf{G}(\Phi(t_n))}_l-\widehat{\mathbf{G}(\Phi_M^n)}_l\right]-iQ_l^{(2)}(\tau)\left[\delta_t^-\widehat{\mathbf{G}(\Phi(t_n))}_l-\delta_t^-\widehat{\mathbf{G}(\Phi_M^n)}_l\right].\tag{C.8}$$

From (C.4) and (C.7), we have

$$|\widehat{\xi}_l^0|\lesssim\int_0^\tau\int_0^s\left|\partial_{s_1}\widehat{\mathbf{G}(\Phi)}_l^0(s_1)\right|ds_1ds.\tag{C.9}$$

By the Parseval equality and assumptions (C) and (D), we get

$$\begin{aligned}\|\mathbf{e}^1(x)\|_{L^2}^2=&\|\xi^0(x)\|_{L^2}^2=(b-a)\sum_{l=-M/2}^{M/2-1}\left|\widehat{\xi}_l^0\right|^2\lesssim(b-a)\tau^2\int_0^\tau\int_0^s\sum_{l=-M/2}^{M/2-1}\left|\partial_{s_1}\widehat{\mathbf{G}(\Phi)}_l^0(s_1)\right|^2ds_1ds\\ \lesssim&\tau^2\int_0^\tau\int_0^s\|\partial_{s_1}(\mathbf{G}(\Phi(s_1)))\|_{L^2}^2\,ds_1ds\lesssim\frac{\tau^4}{\varepsilon^4}\lesssim\frac{\tau^4}{\varepsilon^8}.\end{aligned}\tag{C.10}$$

Thus we have

$$\|\Phi(t_1,x)-\Phi_M^1(x)\|_{L^2}\lesssim h^{m_0}+\|\mathbf{e}^1(x)\|_{L^2}\lesssim h^{m_0}+\frac{\tau^2}{\varepsilon^4}.\tag{C.11}$$

By using the inverse inequality, we get

$$\|\mathbf{e}^1(x)\|_{L^\infty} \le \frac{1}{h^{1/2}}\|\mathbf{e}^1(x)\|_{L^2} \lesssim \frac{\tau^2}{\varepsilon^4 h^{1/2}}, \tag{C.12}$$

which immediately implies

$$\begin{aligned}\|\Phi_M^1(x)\|_{L^\infty} &\le \|\Phi(t_1,x)\|_{L^\infty} + \|\Phi(t_1,x) - P_M\Phi(t_1,x)\|_{L^\infty} + \|\mathbf{e}^1(x)\|_{L^\infty} \\ &\le M_0 + h^{m_0-1} + \frac{\tau^2}{\varepsilon^4 h^{1/2}}.\end{aligned} \tag{C.13}$$

Under the conditions in Theorem 3.1, there exist $h_1 > 0$ and $\tau_1 > 0$ sufficiently small and independent of ε, for $0 < \varepsilon \le 1$, when $0 < h \le h_1$ and $0 < \tau \le \tau_1$, we have

$$\|\Phi_M^1(x)\|_{L^\infty} \le 1 + M_0, \tag{C.14}$$

thus (3.21) is valid when $n = 1$.

Now we assume that (3.21) is valid for all $0 \le n \le m \le \frac{T}{\tau} - 1$, then we need to show that it is still valid when $n = m + 1$. Similar to (C.9) and (C.10), under the assumptions (C) and (D), we obtain

$$|\widehat{\xi_l^n}| \le \int_0^\tau \left(\int_0^s \int_0^{s_1} \left| \partial_{s_2 s_2} \widehat{\mathbf{G}(\Phi)_l^n}(s_2) \right| ds_2 ds_1 + s \int_0^1 \int_{\theta\tau}^\tau \left| \partial_{\theta_1\theta_1} \widehat{\mathbf{G}(\Phi)_l^{n-1}}(\theta_1) \right| d\theta_1 d\theta \right) ds, \tag{C.15}$$

$$\begin{aligned}\|\xi^n(x)\|_{L^2}^2 &= (b-a) \sum_{l=-M/2}^{M/2-1} \left|\widehat{\xi_l^n}\right|^2 \lesssim \tau^3 \int_0^\tau \int_0^s \int_0^{s_1} \sum_{l=-\frac{M}{2}}^{\frac{M}{2}-1} \left| \partial_{s_2 s_2} \widehat{\mathbf{G}(\Phi)_l^n}(s_2) \right|^2 ds_2 ds_1 ds \\ &\quad + \tau^3 \int_0^\tau \int_0^1 \int_{\theta\tau}^\tau s \sum_{l=-\frac{M}{2}}^{\frac{M}{2}-1} \left| \partial_{\theta_1\theta_1} \widehat{\mathbf{G}(\Phi)_l^{n-1}}(\theta_1) \right|^2 d\theta_1 \, d\theta \, ds \\ &\lesssim \tau^6 \|\partial_{tt}(W(\Phi(t)))\|_{L^\infty([0,T];(L^2)^2)}^2 \lesssim \frac{\tau^6}{\varepsilon^8}, \qquad n = 0, 1, \ldots, m.\end{aligned} \tag{C.16}$$

Using the properties of the matrices $Q_l^{(1)}(\tau)$ and $Q_l^{(2)}(\tau)$, it is easy to verify that

$$\|Q_l^{(1)}(\tau)\|_2 \le \tau, \quad \|Q_l^{(2)}(\tau)\|_2 \le \frac{\tau^2}{2}, \quad l = -\frac{M}{2}, \ldots, \frac{M}{2} - 1. \tag{C.17}$$

Combining (C.8) and (C.17), we get

$$\begin{aligned}\frac{1}{b-a}\|R^n(x)\|_{L^2}^2 &= \sum_{l=-M/2}^{M/2-1} |\widehat{R}_l^n|^2 \\ &\lesssim \tau^2 \sum_{l=-M/2}^{M/2-1} \left[\left| \widehat{(\Phi(t_n))}_l - \widehat{(\Phi_M^n)}_l \right|^2 + \left| \widehat{(\Phi(t_{n-1}))}_l - \widehat{(\Phi_M^{n-1})}_l \right|^2 \right. \\ &\quad \left. + \left| \widehat{\mathbf{G}(\Phi)}_l(t_n) - \widehat{\mathbf{G}(\Phi_M^n)}_l \right|^2 + \left| \widehat{\mathbf{G}(\Phi)}_l(t_{n-1}) - \widehat{\mathbf{G}(\Phi_M^{n-1})}_l \right|^2 \right] \\ &\lesssim \tau^2 \left[\|\Phi(t_n,x) - \Phi_M^n(x)\|_{L^2}^2 + \|\Phi(t_{n-1},x) - \Phi_M^{n-1}(x)\|_{L^2}^2 \right] \\ &\lesssim \tau^2 h^{2m_0} + \tau^2 \|\mathbf{e}^n(x)\|_{L^2}^2 + \tau^2 \|\mathbf{e}^{n-1}(x)\|_{L^2}^2, \qquad n = 0, 1, \ldots, m.\end{aligned} \tag{C.18}$$

Multiplying both sides of (C.6) from left by $\left(\widehat{\mathbf{e}}_l^{n+1} + e^{-i\tau\Gamma_l/\varepsilon^2}\widehat{\mathbf{e}}_l^{n}\right)^*$, taking the real parts and using the Cauchy inequality, we obtain

$$\left|\widehat{\mathbf{e}}_l^{n+1}\right|^2 - |\widehat{\mathbf{e}}_l^{n}|^2 \le \tau\left(\left|\widehat{\mathbf{e}}_l^{n+1}\right|^2 + |\widehat{\mathbf{e}}_l^{n}|^2\right) + \frac{|\widehat{R}_l^n|^2}{\tau} + \frac{|\widehat{\xi}_l^n|^2}{\tau}. \tag{C.19}$$

Summing the above for $l = -M/2, \ldots, M/2-1$ and then multiplying it by $(b-a)$, using the Parseval equality, we obtain for $n \ge 1$

$$\left\|\mathbf{e}^{n+1}(x)\right\|_{L^2}^2 - \|\mathbf{e}^{n}(x)\|_{L^2}^2 \lesssim \tau\left(\left\|\mathbf{e}^{n+1}(x)\right\|_{L^2}^2 + \|\mathbf{e}^{n}(x)\|_{L^2}^2\right) + \frac{1}{\tau}\left(\|R^n(x)\|_{L^2}^2 + \|\xi^n(x)\|_{L^2}^2\right). \tag{C.20}$$

Summing (C.20) for $n = 1, \ldots, m$, using (C.18), we derive

$$\left\|\mathbf{e}^{m+1}(x)\right\|_{L^2}^2 - \left\|\mathbf{e}^{1}(x)\right\|_{L^2}^2 \lesssim \tau\sum_{k=1}^{m+1}\left\|\mathbf{e}^{k}(x)\right\|_{L^2}^2 + \frac{m\tau^5}{\varepsilon^8} + m\tau h^{2m_0}, \quad 1 \le m \le \frac{T}{\tau} - 1. \tag{C.21}$$

Noticing $\|\mathbf{e}^1(x)\|_{L^2} \lesssim \frac{\tau^2}{\varepsilon^2} \lesssim \frac{\tau^2}{\varepsilon^4}$ and using the discrete Gronwall's inequality, there exist $0 < \tau_2 \le \frac{1}{2}$ and $h_2 > 0$ sufficiently small and independent of ε such that, for $0 < \varepsilon \le 1$, when $0 < \tau \le \tau_2$ and $0 < h \le h_2$, we get

$$\left\|\mathbf{e}^{m+1}(x)\right\|_{L^2}^2 \lesssim h^{2m_0} + \frac{\tau^4}{\varepsilon^8}, \qquad 1 \le m \le \frac{T}{\tau} - 1. \tag{C.22}$$

Thus we have

$$\|\Phi(t_{m+1}, x) - \Phi_M^{m+1}(x)\|_{L^2} \lesssim h^{m_0} + \|\mathbf{e}^{m+1}(x)\|_{L^2} \lesssim h^{m_0} + \frac{\tau^2}{\varepsilon^4}. \tag{C.23}$$

By using the inverse inequality, we get

$$\|\mathbf{e}^{m+1}(x)\|_{L^\infty} \le \frac{1}{h^{1/2}}\|\mathbf{e}^{m+1}(x)\|_{L^2} \lesssim \frac{\tau^2}{\varepsilon^4 h^{1/2}}, \tag{C.24}$$

which immediately implies

$$\begin{aligned} \|\Phi_M^{m+1}(x)\|_{L^\infty} &\le \|\Phi(t_{m+1}, x)\|_{L^\infty} + \|\Phi(t_{m+1}, x) - P_M\Phi(t_{m+1}, x)\|_{L^\infty} + \|\mathbf{e}^{m+1}(x)\|_{L^\infty} \\ &\le M_0 + h^{m_0-1} + \frac{\tau^2}{\varepsilon^4 h^{1/2}}. \end{aligned} \tag{C.25}$$

Under the conditions in Theorem 3.1, there exist $h_3 > 0$ and $\tau_3 > 0$ sufficiently small and independent of ε, for $0 < \varepsilon \le 1$, when $0 < h \le h_3$ and $0 < \tau \le \tau_3$, we have

$$\|\Phi_M^{m+1}(x)\|_{L^\infty} \le 1 + M_0, \tag{C.26}$$

thus (3.21) is valid when $n = m+1$. Then the proof of (3.21) is completed by the method of mathematical induction under the choice of $h_0 = \min\{h_1, h_2, h_3\}$ and $\tau_0 = \min\{1/2, \tau_1, \tau_2, \tau_3\}$. □

Acknowledgements

We acknowledge support from the Ministry of Education of Singapore grant R-146-000-196-112. Part of this work was done when the authors were visiting the Institute for Mathematical Sciences at the National University of Singapore in 2015.

References

[1] Abanin D A, Morozov S V, Ponomarenko L A, et al. Giant nonlocality near the Dirac point in graphene. Science, 2011, 332: 328–330

[2] Ablowitz M J, Zhu Y. Nonlinear waves in shallow honeycomb lattices. SIAM J Appl Math, 2012, 72: 240–260

[3] Alvarez A. Linearized Crank-Nicholcon scheme for nonlinear Dirac equations. J Comput Phys, 1992, 99: 348–350

[4] Alvarez A, Carreras B. Interaction dynamics for the solitary waves of a nonlinear Dirac model. Phys Lett A, 1981, 86: 327–332

[5] Alvarez A, Kuo P Y, Vázquez L. The numerical study of a nonlinear one-dimensional Dirac equation. Appl Math Comput, 1983, 13: 1–15

[6] Balabane M, Cazenave T, Douady A, et al. Existence of excited states for a nonlinear Dirac field. Commun Math Phys, 1988, 119: 153–176

[7] Balabane M, Cazenave T, Vazquez L. Existence of standing waves for Dirac fields with singular nonlinearities. Commun Math Phys, 1990, 133: 53–74

[8] Bao W, Cai Y. Mathematical theory and numerical methods for Bose-Einstein condensation. Kinet Relat Mod, 2013, 6: 1–135

[9] Bao W, Cai Y. Optimal error estmiates of finite difference methods for the Gross-Pitaevskii equation with angular momentum rotation. Math Comp, 2013, 82: 99–128

[10] Bao W, Cai Y. Uniform and optimal error estimates of an exponential wave integrator sine pseudospectral method for the nonlinear Schrödinger equation with wave operator. SIAM J Numer Anal, 2014, 52: 1103–1127

[11] Bao W, Cai Y, Jia X, Q. Tang. Numerical methods and comparison for the Dirac equation in the nonrelativistic limit regime. arXiv: 1504.02881

[12] Bao W, Cai Y, Zhao X. A uniformly accurate multiscale time integrator pseudospectral method for the Klein-Gordon equation in the nonrelativistic limit regime. SIAM J Numer Anal, 2014, 52: 2488–2511

[13] Bao W, Dong X. Analysis and comparison of numerical methods for the Klein-Gordon equation in the nonrelativistic limit regime. Numer Math, 2012, 120: 189–229

[14] Bao W, Jin S, Markowich P A. On time-splitting spectral approximation for the Schrödinger equation in the semiclassical regime, J. Comput. Phys., 2002, 175: 487-524

[15] Bao W, Jin S, Markowich P A. Numerical study of time-splitting spectral discretizations of nonlinear Schrödinger equations in the semi-classical regimes, SIAM J. Sci. Comput., 2003, 25: 27-64

[16] Bao W, Li X. An efficient and stable numerical method for the Maxwell-Dirac system. J Comput Phys, 2004, 199: 663–687

[17] Bartsch T, Ding Y. Solutions of nonlinear Dirac equations. J Diff Eq, 2006, 226: 210–249

[18] Bechouche P, Mauser N, Poupaud F. (Semi)-nonrelativistic limits of the Dirac eqaution with external time-dependent electromagnetic field. Commun Math Phys, 1998, 197: 405–425

[19] Bournaveas N, Zouraris G E. Split-step spectral scheme for nonlinear Dirac systems. ESAIM: M2AN, 2012 46: 841–874

[20] Brinkman D, Heitzinger C, Markowich P A. A convergent 2D finite-difference scheme for the Dirac-Poisson system and the simulation of graphene. J Comput Phys, 2014, 257: 318–332

[21] Cazenave T, Vazquez L. Existence of localized solutions for a classical nonlinear Dirac field. Commun Math Phys, 1986, 105: 34–47

[22] Chang S J, Ellis S D, Lee B W. Chiral confinement: an exact solution of the massive Thirring model. Phys Rev D, 1975, 11: 3572–2582

[23] Cooper F, Khare A, Mihaila B, et al. Solitary waves in the nonlinear Dirac equation with arbitrary nonlinearity. Phys Rev E, 2010, 82: article 036604

[24] De Frutos J, Sanz-Serna J M. Split-step spectral scheme for nonlinear Dirac systems. J Comput Phys, 1989, 83: 407–423

[25] Dirac P A M. The quantum theory of the electron. Proc R Soc Lond A, 1928, 117: 610–624

[26] Dirac P A M. Principles of Quantum Mechanics. London: Oxford University Press, 1958

[27] Dolbeault J, Esteban M J, Séré E. On the eigenvalues of operators with gaps: Applications to Dirac operator. J Funct Anal, 2000, 174: 208–226

[28] Esteban M J, Séré E. Stationary states of the nonlinear Dirac equation: a variational approach. Commun Math Phys, 1995, 171: 323–350

[29] Esteban M J, Séré E. An overview on linear and nonlinear Dirac equations. Discrete Contin Dyn Syst, 2002, 8: 381–397

[30] Fefferman C L, Weistein M I. Honeycomb lattice potentials and Dirac points. J Amer Math Soc, 2012, 25: 1169–1220

[31] Fefferman C L, Weistein M I. Wave packets in honeycomb structures and two-dimensional Dirac equations. Commun Math Phys, 2014, 326: 251–286

[32] Fillion-Gourdeau F, Lorin E and Bandrauk A D. Resonantly enhanced pair production in a simple diatomic model. Phys. Rev. Lett., 2013, 110: 013002

[33] Fillion-Gourdeau F, Lorin E and Bandrauk A D. A split-step numerical method for the time-dependent Dirac equation in 3-D axisymmetric geometry. J. Comput. Phys., 2014, 272: 559-587

[34] Finkelstein R, Lelevier R, Ruderman M. Nonlinear spinor fields. Phys Rev, 1951, 83: 326–332

[35] Foldy L L, Wouthuysen S A. On the Dirac theory of spin 1/2 particles and its nonrelavistic limit. Phys Rev, 1950, 78: 29–36

[36] Fushchich W I, Shtelen W M. On some exact solutions of the nonlinear Dirac equation. J. Phys A: Math Gen, 1983, 16: 271–277

[37] Gautschi W. Numerical integration of ordinary differential equations based on trigonometric polynomials. Numer Math, 1961, 3: 381–397

[38] Grigore D R, Nenciu G, Purice R. On the nonrelativistic limits of the Dirac Hamiltonian. Ann Inst Henri Poincaré, 1989, 51: 231–263
[39] Haddad L H, Carr L D. The nonlinear Dirac equation in Bose-Einstein condensates: foundation and symmetries. Physica D, 2009, 238: 1413–1421
[40] Haddad L H, Weaver C M, Carr L D. The nonlinear Dirac equation in Bose-Einstein condensates: I. Relativistic solitons in armchair nanoribbon optical lattices. arXiv: 1305.6532
[41] Hagen C R. New solutions of the Thirring model. Nuovo Cimento, 1967, 51: 169–186
[42] Hairer E, Lubich Ch, Wanner G. Geometric Numerical Integration. Springer-Verlag, 2002.
[43] Hammer R, Pötz W, Arnold A. A dispersion and norm preserving finite difference scheme with transparent boundary conditions for the Dirac equation in (1+1)D. J Comput Phys, 2014, 256: 728–747
[44] Heisenberg W. Quantum theory of fields and elementary particles. Rev Mod Phys, 1957, 29: 269–278
[45] Ivanenko D D. Notes to the theory of interaction via particles. Zh. Eksp. Teor. Fiz., 1938, 8: 260-266
[46] Hong J L, Li C. Multi-symplectic Runge-Kutta methods for nonlinear Dirac equations. J Comput Phys, 2006, 211: 448–472
[47] Huang Z, Jin S, Markowich P A, et al. A time-splitting spectral scheme for the Maxwell-Dirac system. J Comput Phys, 2005, 208: 761–789
[48] Hunziker W. On the nonrelativistic limit of the Dirac theory. Commun Math Phys, 1975, 40: 215–222
[49] Komech A, Komech A. Golbal attraction to solitary waves for a nonlinear Dirac equation with mean field interaction. SIAM J Math Anal, 2010, 42: 2944–2964
[50] Korepin V E. Dirac calculation of the S matrix in the massive Thirring model. Theor Math Phys, 1979, 41: 953–967
[51] Lee S Y, Kuo T K, Gavrielides A. Exact localized solutions of two-dimensional field theories of massive fermions with Fermi interactions. Phys Rev D, 1975, 12: 2249–2253
[52] Liang H, Meng J, Zhou S-G. Hidden pseudospin and spin symmetries and their origins in atomic nuclei. Phys. Reports, 2015, 570: 1–84
[53] Lubich Ch. On splitting methods for Schrödinger-Poisson and cubic nonlinear Schrödinger equations. Math Comp, 2008, 77: 2141–2153
[54] Masmoudi N, Mauser N J. The selfconsistent Pauli equaiton. Monatsh Math, 2001, 132: 19–24
[55] Mathieu P. Soliton solutions for Dirac equations with homogeneous non-linearity in (1+1) dimensions. J Phys A: Math Gen, 1985, 18: L1061-L1066
[56] Merkl M, Jacob A, Zimmer F E, et al. Chiral confinement in quasirelativistic Bose-Einstein condensates. Phys Rev Lett, 2010, 104: article 073603
[57] Merle F. Existence of stationary states for nonlinear Dirac equations. J Diff Eq, 1988, 74: 50–68
[58] Najman B. The nonrelativistic limit of the nonlinear Dirac equation. Ann Inst Henri Poincaré, 1992, 9: 3–12
[59] Neto A H C, Guinea F, Peres N M R, et al. The electronic properties of the graphene. Rev Mod Phys, 2009, 81: 109–162
[60] Nraun J W, Su Q, Grobe R. Numerical approach to solve the time-dependent Dirac equation. Phys Rev A, 1999, 59: 604–612
[61] Rafelski J. Soliton solutions of a selfinteracting Dirac field in three space dimensions. Phys Lett B, 1977, 66: 262–266
[62] Ring P. Relativistic mean field theory in finite nuclei. Prog. Part. Nucl. Phys., 1996, 37: 193–263
[63] Saha B. Nonlinear spinor fields and its role in cosmology. Int J Theor Phys, 2012, 51: 1812–1837
[64] Shao S H, Quintero N R, Mertens F G, Cooper F, Khare A, Saxena A. Stability of solitary waves in the nonlinear Dirac equation with arbitrary nonlinearity. Phys Rev E, 2014, 90, 032915
[65] Shao S H, Tang H Z. Interaction for the solitary waves of a nonlinear Dirac model. Phys Lett A, 2005, 345: 119–128
[66] Shao S H, Tang H Z. Higher-order accurate Runge-Kutta discontinuous Galerkin methods for a nonlinear Dirac model. Discrete Cont Dyn Syst B, 2006, 6: 623–640
[67] Shao S H, Tang H Z. Interaction of solitary waves with a phase shift in a nonlinear Dirac model. Commun Comput Phys, 2008, 3: 950–967
[68] Shen J, Tang T. Spectral and High-Order Methods with Applications. Beijing: Science Press, 2006
[69] Soler M. Classical, stable, nonlinear spinor field with positive rest energy. Phys Rev D, 1970, 1: 2766–2769
[70] Strang G. On the construction and comparision of difference schemes. SIAM J Numer Anal, 1968, 5: 505–517
[71] Stubbe J. Exact localized solutions of a family of two-dimensional nonliear spinor fields. J Math Phys, 1986, 27: 2561–2567
[72] Takahashi K. Soliton solutions of nonlinear Dirac equations. J Math Phys, 1979, 20: 1232–1238
[73] Thirring W E. A soluble relativistic field theory. Ann Phys, 1958, 3: 91–112
[74] Veselic K. Perturbation of pseudoresolvents and analyticity in $1/c$ of relativistic quantum mechanics. Commun Math Phys, 1971, 22: 27–43
[75] Wang Z Q, Guo B Y. Modified Legendre rational spectral method for the whole line. J Comput Math, 2004, 22: 457–472
[76] Wang H, Tang H Z. An efficient adaptive mesh redistribution method for a nonlinear Dirac equation. J Comput Phys, 2007, 222: 176–193
[77] Werle J. Non-linear spinor equations with localized solutions. Lett Math Phys, 1977, 2: 109–114
[78] White G B. Splitting of the Dirac operator in the nonrelativistic limit. Ann Inst Henri Poincaré, 1990, 53: 109–121
[79] Xu J, Shao S H, Tang H Z. Numerical methods for nonlinear Dirac equation. J Comput Phys, 2013, 245: 131–149
[80] Xu J, Shao S H, Tang H Z, Wei D Y. Multi-hump solitary waves of a nonlinear Dirac equation. Commun. Math. Sci, 2015, Vol. 13, No. 5: 1219-1242